Thallium(I) Sandwich, Multidecker, and Ether Complexes Stabilized by Weakly-Coordinating Anions: A Spectroscopic, Structural, and Theoretical Investigation

ARTICLE *in* JOURNAL OF THE AMERICAN CHEMICAL SOCIETY · FEBRUARY 2007

Impact Factor: 12.11 · DOI: 10.1021/ja0657105 · Source: PubMed

J|A|C|S
ARTICLES
Published on Web 01/09/2007

Thallium(I) Sandwich, Multidecker, and Ether Complexes Stabilized by Weakly-Coordinating Anions: A Spectroscopic, Structural, and Theoretical Investigation

Yann Sarazin,[†] David L. Hughes,[†] Nikolas Kaltsoyannis,[‡] Joseph A. Wright,[†] and Manfred Bochmann*,[†]

Contribution from the Wolfson Materials and Catalysis Centre, School of Chemical Sciences and Pharmacy, University of East Anglia, Norwich NR4 7TJ, U.K., and Department of Chemistry, University College London, 20 Gordon Street, London WC1H 0AJ, U.K.

Received August 15, 2006; E-mail: m.bochmann@uea.ac.uk

Abstract: The reaction of thallium ethoxide with $[H(OEt_2)_2][H_2N\{B(C_6F_5)_3\}_2]$ in diethyl ether afforded $[Tl(OEt_2)_3][H_2N\{B(C_6F_5)_3\}_2]$ (**2a**), $[Tl(OEt_2)_4][H_2N\{B(C_6F_5)_3\}_2]$ (**2b**), or $[Tl(OEt_2)_2][H_2N\{B(C_6F_5)_3\}_2]\cdot CH_2Cl_2$ (**2c**), depending on the reaction conditions. The dication in the hydrolysis product $[Tl_4(\mu^3\text{-}OH)_2][H_2N\{B(C_6F_5)_3\}_2]_2\cdot 4CH_2Cl_2$ consists of two bridging and two terminal Tl^+ ions bound to triply bridging hydroxides. Heating Et_2O complexes in toluene afforded $[Tl(\eta^6\text{-toluene})_n][H_2N\{B(C_6F_5)_3\}_2]$ (**4**, $n = 2, 3$), while C_6Me_6 addition gave the first thallium−C_6Me_6 adduct, $[Tl(\eta^6\text{-}C_6Me_6)_2][H_2N\{B(C_6F_5)_3\}_2]\cdot 1.5CH_2Cl_2$ (**5a**), a bent sandwich complex with very short Tl···centroid distances. These arene complexes show no close contacts between cations and anions. Displacement of toluene ligands by ferrocene gave $[Tl_2(FeCp_2)_3][H_2N\{B(C_6F_5)_3\}_2]_2\cdot 5CH_2Cl_2$ (**6**) which contains the multidecker cations $[Tl(FeCp_2)]^+$ and $[Tl(FeCp_2)_2]^+$ in a 1:1 ratio. By contrast, decamethylferrocene leads to electron transfer; the isolable thallium−ferrocene complexes may therefore be viewed as precursor complexes for this redox step. With 18-crown-6 the complexes $[Tl(18\text{-crown-}6)_2][H_2N\{B(C_6F_5)_3\}_2]$ (**11a**) and $[Tl(18\text{-crown-}6)][H_2N\{B(C_6F_5)_3\}_2]\cdot 2CH_2Cl_2$ (**11b**) were isolated. The structure of the latter shows an eight-coordinate thallium ion, where the coordination to the six oxygen donors in equatorial positions is completed by axial contacts to two F atoms of the counter anions. The bonding between thallium(I) and arenes was explored by density-functional theory (DFT) calculations. The optimized geometry of $[Tl(tol)_3]^+$ converged to a structure very similar to that obtained experimentally. Calculations on $[Tl(C_6Me_6)_2]^+$ (**5b**) to establish whether a linear or bent geometry is the most stable revealed a very flat potential-energy surface for distortions of the Ctr(3)−Tl−Ctr(4) angle. Overall, there is very little energetic preference for one particular geometry over another above about 140°, in good agreement with the crystallographic geometry. The calculated Tl−arene interaction energies increase from 73.7 kJ mol^{-1} for toluene to 121.7 kJ mol^{-1} for C_6Me_6.

Thallium salts of more or less weakly coordinating anions are a convenient way to abstract halide ligands and are therefore widely employed in ligand exchange reactions and to generate coordinatively unsaturated metal complexes. Some time ago we reported the synthesis of $[H_2N\{B(C_6F_5)_3\}_2]^-$,[1] a readily prepared and stable amidodiborate anion which can be used to support a variety of electrophilic metal centers and catalysts.[2−4] Moreover, we found that this anion frequently offers better crystallization properties than $[B(C_6F_5)_4]^-$. In the course of studies on the synthesis of heavy-metal salts of such anions, we have investigated the chemistry of thallium(I) and report here the syntheses, structures, and coordination modes of new families of thallium(I) arene and ether complexes where the counteranion exerts only a minimal influence on the coordination geometry.

In contrast to transition-metal arene complexes, arene π-complexes of monovalent p-block metals are rather scarce.[5] Structural reports on thallium(I) arene complexes have only appeared in the literature in the last 20 years. Amma et al. demonstrated the existence of $(C_6H_6)_2\cdot TlAlCl_4$ and $C_6H_6\cdot 2(TlAlCl_4)$ in the late 1960s,[6] but these compounds were only characterized by elemental analysis. It was not until 1985 that Schmidbaur isolated the first structurally characterized Tl(I) arene complex, $[(mes)_6Tl_4][GaBr_4]_4$,[7] which consists of a tetrameric $[TlGaBr_4]_4$ framework where two $Tl(mes)^+$ and two $Tl(mes)_2^+$ cations (mes = mesitylene, 1,3,5-$C_6H_3Me_3$) are bridged by four $[GaBr_4]^-$ anions in a complicated pattern of Tl···Br contacts. η^6-Coordination of the mesitylene molecules was found for both

[†] University of East Anglia.
[‡] University College London.

(1) Lancaster, S. J.; Rodriguez, A.; Lara-Sanchez, A.; Hannant, M. D.; Walker, D. A.; Hughes, D. L.; Bochmann, M. *Organometallics* **2002**, *21*, 451−453.
(2) Farrow, E.; Sarazin, Y.; Hughes, D. L.; Bochmann, M. *J. Organomet. Chem.* **2004**, *689*, 4624−4629.
(3) Hannant, M. D.; Schormann, M.; Bochmann, M. *J. Chem. Soc., Dalton Trans.* **2002**, 4071−4073.
(4) Hannant, M. D.; Schormann, M.; Hughes, D. L.; Bochmann, M. *Inorg. Chim. Acta* **2005**, *358*, 1683−1691.
(5) Schmidbaur, H. *Angew. Chem., Int. Ed. Engl.* **1985**, *24*, 893−904.
(6) Auel, T.; Amma, E. L. *J. Am. Chem. Soc.* **1968**, *90*, 5941−5942.
(7) Schmidbaur, H.; Bublak, W.; Riede, J.; Müller, G. *Angew. Chem., Int. Ed. Engl.* **1985**, *24*, 414−415.

Scheme 1. Synthesis of Thallium Diethyl Ether Complexes $[Tl(OEt_2)_n][H_2N\{B(C_6F_5)_3\}_2]$ ($n = 3$, **2a**; $n = 4$, **2b**) and $[Tl(OEt_2)_2][H_2N\{B(C_6F_5)_3\}_2]\cdot CH_2Cl_2$ (**2c**)

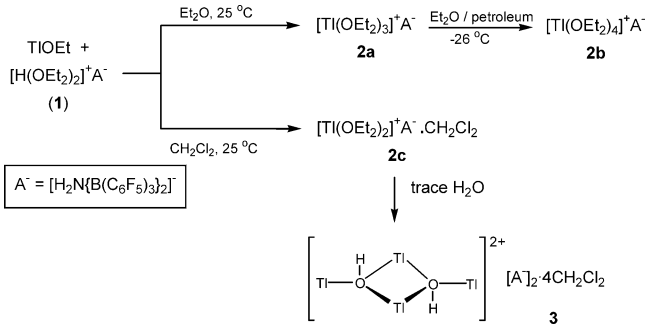

types of cation, with Tl···centroid distances between 2.94 and 3.03 Å. Schmidbaur's initial discovery was rapidly followed by Strauss' characterization of $[TlOTeF_5(mes)_2]_2\cdot$mes and $[Tl(mes)_2][B(OTeF_5)_4]$,[8,9] two complexes where the mesitylene molecules are also η^6-coordinated to the metal ions with Tl···C_{arene} distances in the regions of 3.12−3.52 and 3.12−3.22 Å respectively. Hawthorne described the structure of $Tl[Al(C_2B_9H_{11})_2]\cdot{}^2/_3$toluene (Tl···$C_{arene}$ = 3.17−3.23 Å),[10] while Schmidbaur reported that the reaction of [2.2]paracyclophane and $Tl[GaCl_4]$ in toluene yields the complex $[Tl(p\text{-}C_6H_4CH_2CH_2)_2][GaCl_4]$,[11] with one-dimensional Tl···(p-$C_6H_4CH_2CH_2$)···Tl···(p-$C_6H_4CH_2CH_2$) stacks formed via η^6-coordination of the outer side of the benzene rings to the thallium atoms (Tl···centroid = 2.95 Å). Frank and co-workers characterized three dimeric complexes $[Tl(arene)_2(MCl_4)]_2$ (M = Al, arene = mesitylene, 1,2,4-trimethylbenzene; M = Ga, arene = 1,2,4-trimethylbenzene) which all exhibit Tl···C_{arene} distances in the range of 3.23−3.41 Å.[12,13] Finally, Reed prepared $[Tl(toluene)_2][CB_{11}H_6Br_6]$, a complex dimer in the solid state which features two halocarborane bridges and η^6-coordination of the toluene molecules (Tl···C_{arene} = 3.21−3.50 Å).[14] In addition to these salts, there are also several cases of *intra*molecular Tl(I)···arene interactions, that is, where the arene is part of a ligand framework covalently bound to the metal.[15−25] All these thallium(I) arene adducts display significant stabilizing Tl···X (X = halogen or oxygen) interactions with the counteranion which profoundly influence the thallium coordination geometry and the structure of the salts in the solid state.[6−14]

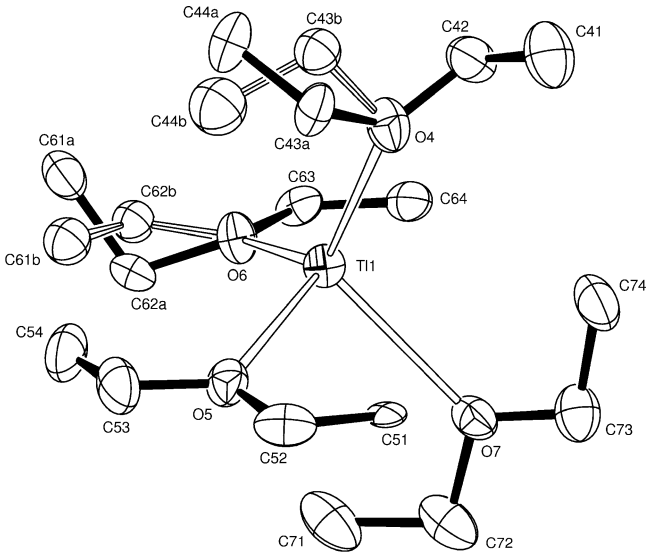

Figure 1. View of the principal Tl atom and its ligands of the cation in **2b** indicating the atom numbering scheme and disordered groups. Thermal ellipsoids are drawn at the 30% probability level. Hydrogen atoms are omitted for clarity. Selected bond lengths (Å) and bond angles (deg): Tl(1)−O(4) = 2.847(4), Tl(1)−O(5) = 2.870(4), Tl(1)−O(6) = 2.850(4), Tl(1)−O(7) = 2.797(4); O(4)−Tl(1)−O(5) = 86.92(12), O(6)−Tl(1)−O(4) = 132.97(12), O(7)−Tl(1)−O(4) = 110.52(12), O(6)−Tl(1)−O(5) = 123.65(11), O(7)−Tl(1)−O(5) = 92.49(11), O(7)−Tl(1)−O(6) = 103.41(12).

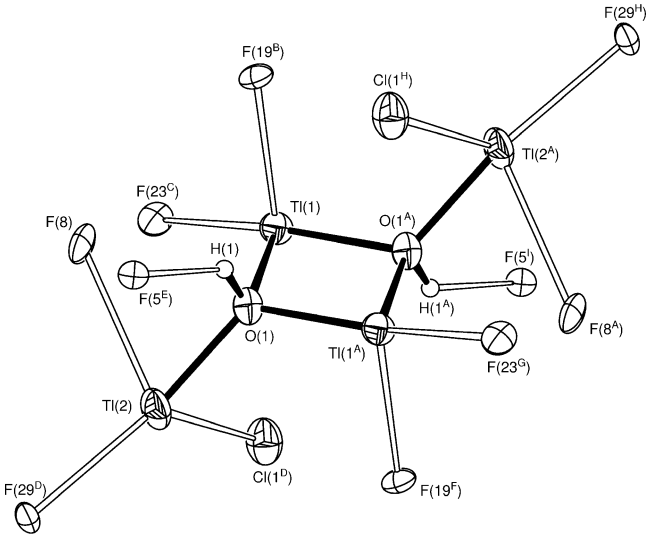

Figure 2. View of the dicationic $[Tl_4(\mu^3\text{-}OH)_2]^{2+}$ core in **3**. Thermal ellipsoids are shown at the 50% probability level. Selected bond lengths (Å) and bond angles (deg): Tl(1)−O(1) = 2.526(3), Tl(1)−O(1^A) = 2.483(3), Tl(1)−F(19^B) = 3.045(3), Tl(1)−F(23^C) = 3.101(3), Tl(2)−O(1) = 2.398(3), Tl(2)−F(8) = 3.143(3), Tl(2)−F(29^D) = 3.025(3), Tl(2)−Cl(1^D) = 3.269(2), O(1)−H(1) = 0.98, H(1)···F(5^E) = 2.30, O(1)···F(5^E) = 3.076(4); O(1)−Tl(1)−O(1^A) = 77.77(10), O(1)−Tl(1)−F(19^B) = 91.98(10), O(1)−Tl(1)−F(23^C) = 119.76(9), O(1^A)−Tl(1)−F(19^B) = 93.52(10), O(1^A)−Tl(1)−F(23^C) = 154.24(10), F(19^B)−Tl(1)−F(23^C) = 103.82(7), O(1)−Tl(2)−F(8) = 66.70(9), O(1)−Tl(2)−F(29^D) = 159.85(10), O(1)−Tl(2)−Cl(1^D) = 78.63(9), F(8)−Tl(2)−F(29^D) = 106.58(8), F(8)−Tl(2)−Cl(1^D) = 109.39(6), F(29^D)−Tl(2)−Cl(1^D) = 121.09(6), Tl(1)−O(1)−Tl(1^A) = 102.23(10), Tl(1)−O(1)−Tl(2) = 117.87(15), Tl(1^A)−O(1)−Tl(2) = 121.23(14), Tl(1)−O(1)−H(1) = 104.6, Tl(1^A)−O(1)−H(1) = 104.6, Tl(2)−O(1)−H(1) = 104.6, O(1)−H(1)···F(5^E) = 136.

(8) Strauss, S. H.; Noirot, M. D.; Anderson, O. P. *Inorg. Chem.* **1986**, *25*, 3850−3851.
(9) Noirot, M. D.; Anderson, O. P.; Strauss, S. H. *Inorg. Chem.* **1987**, *26*, 2216−2223.
(10) Bandman, M. A.; Knobler, C. B.; Hawthorne, M. F. *Inorg. Chem.* **1988**, *27*, 2399−2400.
(11) Schmidbaur, H.; Bublak, W.; Huber, B.; Hofmann, J.; Müller, G. *Chem. Ber.* **1989**, *122*, 265−270.
(12) Frank, W.; Korrell, G.; Reiβ, G. J. *Z. Anorg. Allg. Chem.* **1995**, *621*, 765−770.
(13) Frank, W.; Korrell, G.; Reiβ, G. J. *J. Organomet. Chem.* **1996**, *506*, 293−300.
(14) Mathur, R. S.; Drovetskaya, T.; Reed, C. A. *Acta Crystallogr.* **1997**, *C53*, 881−883.
(15) Beck, J.; Sträle, J. *Z. Naturforsch., B: Chem. Sci.* **1986**, *41*, 1381−1386.
(16) Frank, W.; Kuhn, D.; Müller-Becker, S.; Ravazi, A. *Angew. Chem., Int. Ed. Engl.* **1993**, *32*, 90−92.
(17) Waezsada, S. D.; Belgardt, T.; Noltemeyer, M.; Roesky, H. W. *Angew. Chem., Int. Ed. Engl.* **1994**, *33*, 1351−1352.
(18) Hellman, K. W.; Galka, C. H.; Gade, L. H.; Steiner, A.; Wright, D. S.; Kottke, T.; Stalke, D. *Chem. Commun.* **1998**, 549−550.
(19) Galka, C. H.; Gade, L. H. *Inorg. Chem.* **1999**, *38*, 1038−1039.
(20) Kristansson, O. *Eur. J. Inorg. Chem.* **2002**, 2355−2361.
(21) Wiesbrock, F.; Schmidbaur, H. *J. Am. Chem. Soc.* **2003**, *125*, 3622−3630.
(22) Kunrath, F. A.; Casagrande, O. L., Jr.; Toupet, L.; Carpentier, J.-C. *Eur. J. Inorg. Chem.* **2004**, 4803−4806.
(23) Wright, R. J.; Brynda, M.; Power, P. P. *Inorg. Chem.* **2005**, *44*, 3368−3370.
(24) Rasika Dias, H. V.; Singh, S.; Cundari, T. R. *Angew. Chem., Int. Ed. Engl.* **2005**, *44*, 4907−4910.
(25) Fox, A. R.; Wright, R. J.; Rivard, E.; Power, P. P. *Angew. Chem., Int. Ed. Engl*. **2005**, *44*, 7729−7733.

Scheme 2. Synthetic Pathways to Structurally Characterized Thallium(I)−Arene Complexes

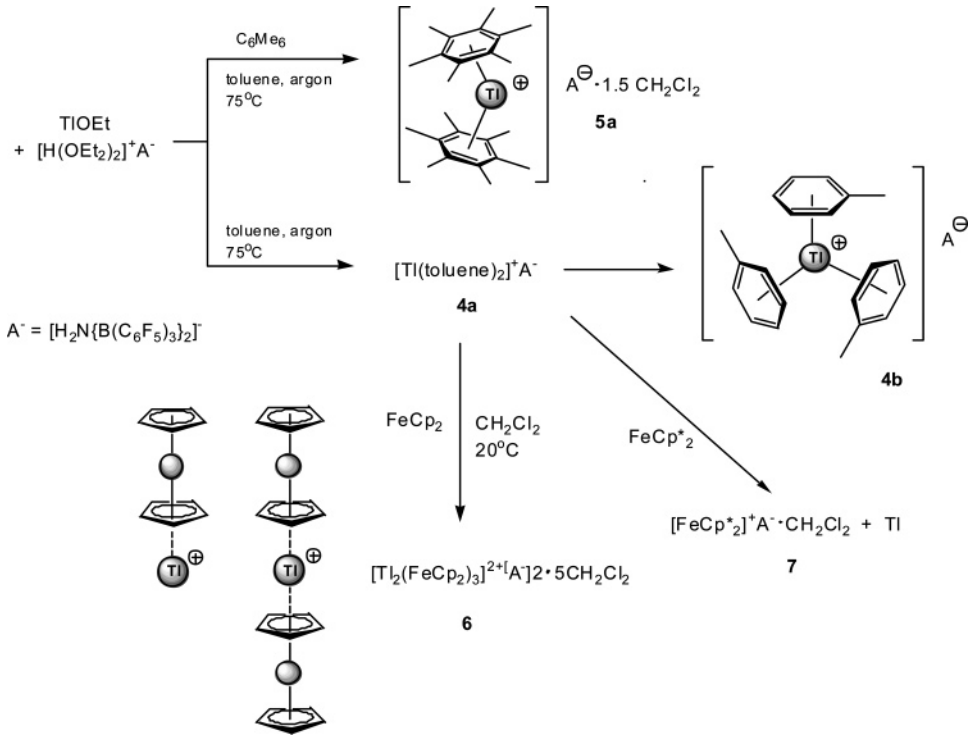

We report here the preparation and crystallographic characterization of the new Tl(I) arene complexes $[Tl(toluene)_3][H_2N\{B(C_6F_5)_3\}_2]$ and $[Tl(C_6Me_6)_2][H_2N\{B(C_6F_5)_3\}_2]\cdot 1.5CH_2Cl_2$ which, unlike previously reported examples, display $[Tl(arene)_n]^+$ ions free of bonding contacts to the counteranion.

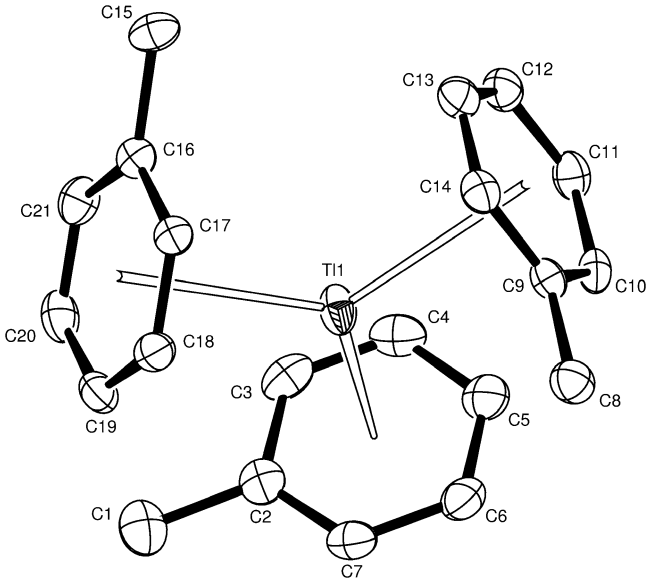

Figure 3. ORTEP diagram of the cationic component of **4b**, showing the atomic numbering scheme. Thermal ellipsoids are drawn at the 50% probability level; hydrogen atoms have been omitted for clarity. Selected bond lengths (Å) and bond angles (deg): Tl(1)−Ctr(1) = 3.010, Tl(1)−Ctr(2) = 2.947, Tl(1)−Ctr(3) = 2.942, Tl(1)−C(2) = 3.346(5), Tl(1)−C(3) = 3.283(5), Tl(1)−C(4) = 3.273(5), Tl(1)−C(5) = 3.307(5), Tl(1)−C(6) = 3.333(5), Tl(1)−C(7) = 3.339(5), Tl(1)−C(9) = 3.256(4), Tl(1)−C(10) = 3.158(4), Tl(1)−C(11) = 3.163(4), Tl(1)−C(12) = 3.261(5), Tl(1)−C(13) = 3.354(5), Tl(1)−C(14) = 3.339(4), Tl(1)−C(16) = 3.307(4), Tl(1)−C(17) = 3.229(4), Tl(1)−C(18) = 3.185(4), Tl(1)−C(19) = 3.205(4), Tl(1)−C(20) = 3.273(5), Tl(1)−C(21) = 3.316(5); Ctr(1)−Tl(1)−Ctr(2) = 120.7, Ctr(1)−Tl(1)−Ctr(3) = 125.3, Ctr(2)−Tl(1)−Ctr(3) = 113.7.

Some of the $Tl^+\cdots$arene interactions in these compounds are the strongest reported to date. The nature of arene bonding was investigated by molecular orbital calculations, and ^{205}Tl NMR chemical shifts are shown to provide clear information on the coordination environment of thallium. The reaction with ferrocene gives the multidecker complex $[Tl_2(FeCp_2)_3][H_2N\{B(C_6F_5)_3\}_2]_2\cdot 5CH_2Cl_2$. The $[Tl(arene)_n]^+$ salts undergo a number of ligand exchange reactions leading to new types of arene and ether complexes.

Results and Discussion

Syntheses and Characterization. The protolysis of thallium ethoxide by the strong Brønsted acid $[H(OEt_2)_2][H_2N\{B(C_6F_5)_3\}_2]$[1] (**1**) in diethyl ether yielded a white solid (Scheme 1). The spectroscopic data were consistent with the formulation $[Tl(OEt_2)_3][H_2N\{B(C_6F_5)_3\}_2]$ (**2a**, yield 70%). The ^{19}F NMR spectrum showed three resonances at δ −133.5, −160.6, and −166.0, typical of a solvent-separated perfluorinated amidodiborate anion, and its ^{11}B NMR resonance was observed at δ −5.37. The ^1H NMR spectrum suggested the presence of three molecules of diethyl ether per thallium atom, and this was confirmed by the elemental analysis.

Compound **2a** is very soluble in Et_2O and CH_2Cl_2 but is only sparingly soluble in aromatic hydrocarbons at room temperature and insoluble in light petroleum. It is noteworthy that unlike $Tl[B\{3,5\text{-}C_6H_3(CF_3)_2\}_4]$[26] and $Tl[B(C_6F_5)_4]$,[27] the thallium(I) salt of the amidodiborate could not be obtained free of Et_2O since the solvent molecules could not be removed even upon gentle heating under vacuum. X-ray quality crystals were obtained as colorless blocks upon recrystallization of **2a** in a diethyl ether/light petroleum mixture at −26 °C; however, the molecular structure showed a complex with four Et_2O molecules per metal

(26) Hughes, R. P.; Lindner, D. C.; Rheingold, A. L.; Yap, G. P. A. *Inorg. Chem.* **1997**, *36*, 1726−1727.
(27) Alberti, D.; Pörschke, K.-R. *Organometallics* **2004**, *23*, 1459−1460.

Table 1. Comparative Data for Tl(I)−Arene Complexes

compound	A[a]	$Tl^{+\cdot\cdot\cdot}$–A interaction	closest Tl···A distance [Å]	Tl···Ctr[b] [Å]	Tl···C_{ring} [Å]	ref
4b	$H_2N\{B(C_6F_5)_3\}_2$	no	3.43	3.01	3.27−3.35	this work
				2.95	3.16−3.35	
				2.94	3.18−3.32	
5b	$H_2N\{B(C_6F_5)_3\}_2$	no	3.53	2.79	3.11−3.15	this work
			3.55	2.85	3.15−3.20	
6	$H_2N\{B(C_6F_5)_3\}_2$	yes	3.03	2.92	3.07−3.26	this work
			3.26	2.93	3.05−3.28	
			3.18			
$[Tl_4(mes)_6][A]_4$[c]	$GaBr_4$	yes	3.35	2.94		7
				3.01		
				3.03		
$[Tl(A)(mes)_2]_2\cdot mes$[c]	$OTeF_5$	yes	2.69		3.35−3.43	8
			2.70		3.13−3.52	
$[Tl(mes)_2][A]$[c]	$B(OTeF_5)_4$	yes	2.69		3.12−3.22	9
			2.70		3.14−3.21	
			2.71			
$Tl[A]\cdot{}^2/_3tol$[d]	$Al(C_2B_9H_{11})_2$	yes	2.75		3.17−3.24	10
			2.79			
$[Tl(pcp)_2][A]$[e]	$GaCl_4$	yes	3.28	2.95	3.16−3.44	11
			3.37			
$[Tl(mes)_2]_2[A]_2$	$AlCl_4$	yes	3.21	2.94	3.16−3.34	12
			3.29	3.01	3.25−3.39	
$[Tl(tmb)_2]_2[A]_2$[f]	$AlCl_4$	yes	3.36	2.96	3.23−3.29	13
			3.34	3.06	3.30−3.41	
$[Tl(tmb)_2]_2[A]_2$[f]	$GaCl_4$	yes	3.33	2.97	3.25−3.30	13
				3.07	3.30−3.41	
$[Tl(tol)_2][A]$[d]	$CB_{11}H_6Br_6$	yes	3.39	2.99	3.21−3.35	14
			3.42	3.09	3.27−3.50	
			3.59			

[a] A = anion. [b] Ctr = centroid. [c] mes = 1,3,5-$Me_3C_3H_6$. [d] tol = toluene. [e] pcp = [2,2]paracyclophane. [f] tmb = 1,3,4-$Me_3C_3H_6$.

center rather than three, $[Tl(OEt_2)][H_2N\{B(C_6F_5)_3\}_2]$ (**2b**). Evidently, **2b** was obtained as the least soluble product of the crystallization which loses a ligand upon drying under vacuum to yield **2a**.

In an attempt to improve the yield of the synthesis of **2a**, the reaction of **1** and TlOEt was carried out in dichloromethane at room temperature. A very fine white powder was obtained, and characterization by NMR and microanalysis unambiguously confirmed the composition $[Tl(OEt_2)_2][H_2N\{B(C_6F_5)_3\}_2]\cdot CH_2Cl_2$ (**2c**). The solution NMR spectroscopic data of the two compounds are essentially identical. Crystals of **2c** could not be obtained; however, storing a concentrated dichloromethane solution of **2c** at −26 °C for several days gave colorless blocks of a hydrolysis product, $[Tl_4(\mu^3\text{-}OH)_2][H_2N\{B(C_6F_5)_3\}_2]_2\cdot 4CH_2Cl_2$ (**3**) in low yield, which were identified by X-ray crystallography. Owing to the very poor solubility in chlorinated solvents, NMR spectroscopic data could not be obtained. The IR spectrum exhibited the characteristic OH and NH_2 bands at 3610 and 3565 (OH) and 3384 and 3345 cm^{-1} (NH_2).

The solid-state structures of the cations in **2b** and **3** are shown in Figures 1 and 2, respectively. To the best of our knowledge, **2b** represents the first example of a structurally characterized thallium(I)-diethyl ether complex.

There is disorder in the cationic component. The thallium atom is disordered over three sites in the ratio ca. 85.0:11.5:3.5. In the principal Tl atom site, the metal is coordinated by four ether molecules in a distorted tetrahedral arrangement. The lone pair of electrons is not stereochemically active.

The ligands of the Tl atoms in the minor occupancy sites were not resolved, but O(5) and O(6) are at reasonable distances from Tl(2) so that these ligands may be common to both Tl(1) and Tl(2). The ether ligands of O(5) and O(7) are ordered in the normal all-trans conformation, whereas one ethyl group in each of the ligands of O(4) and O(6) has alternative sites.

The thallium−oxygen bond lengths in the principal component are in the range 2.797−2.870 Å, with the Tl(1)−O(7) distance of 2.797(4) Å slightly shorter than the remaining three. They are only marginally longer than the thallium−O(THF) distances found in $[(THF)_2Tl(\mu\text{-}NC)Mn(CO)(Ph_2PCH_2PPh_2)_2][PF_6]$ [Tl−O = 2.74(3)−2.75(3) Å][28] and in Tl(tetraphenylporphyrinato)(OSO_2CF_3)(THF)·THF [Tl−O = 2.778(7) Å].[29]

The structure of the $[H_2N\{B(C_6F_5)_3\}_2]^-$ anion in **2b** is well resolved and resembles that of the already reported $[Na(OEt_2)_4][H_2N\{B(C_6F_5)_3\}_2]$.[1] The geometry is bent, with N(1)−B(1) and N(1)−B(2) bond distances of 1.629(6) and 1.636(6) Å, respectively, and a B(1)−N(1)−B(2) angle of 134.1(4)°. The anion is stabilized by four substantial N−H···F hydrogen bonds which range from 2.00(6) to 2.27(7) Å; the shortest is slightly longer than that found in $[Na(OEt_2)_4][H_2N\{B(C_6F_5)_3\}_2]$ (1.90 Å).

The unit cell of **3** consists of the $[Tl_4(\mu^3\text{-}OH)_2]^{2+}$ dication and two $[H_2N\{B(C_6F_5)_3\}_2]^-$ anions; it also contains four CH_2Cl_2 molecules which have been refined freely. The structure of the cation, shown in Figure 2, has a central $Tl_2(OH)_2$ core lying about a center of symmetry; both oxygen atoms O(1) and O(1^A) are coordinated to the two bridging thallium atoms [Tl(1) and Tl(1^A)] and to a terminal Tl atom [Tl(2) and Tl(2^A), respectively]. The location of the hydroxyl hydrogen atom was estimated from the final refined atom parameters. The O−Tl

(28) Connelly, N. J.; Hicks, O. M.; Lewis, G. R.; Moreno, M. T.; Orpen, A. G. *Dalton Trans.* **1998**, 1913−1918.
(29) Tung, J.-Y.; Chen, J.-H.; Liao, F.-L.; Wang, S.-L.; Hwang, L.-P. *Inorg. Chem.* **1998**, *37*, 6104−6108.

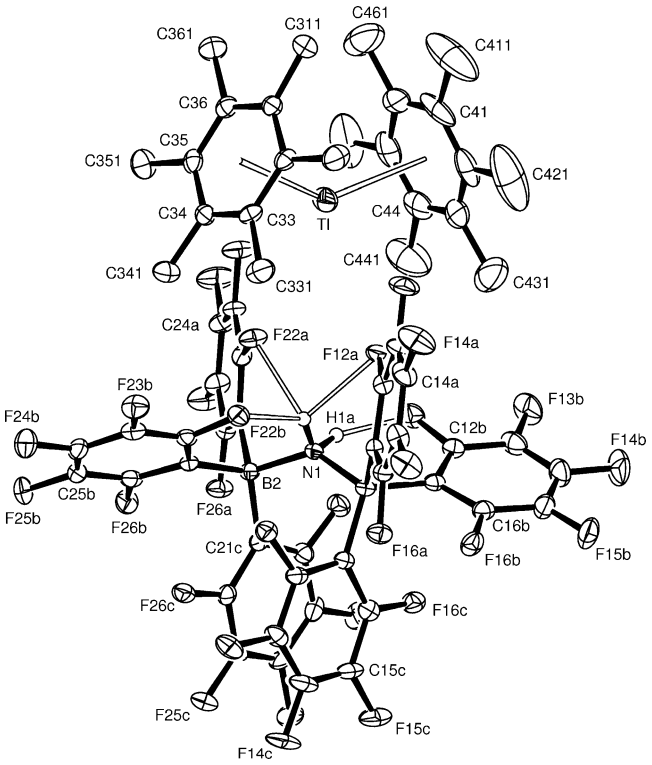

Figure 4. ORTEP diagram of **5b** indicating the numbering scheme and the relative positions of the ions. Thermal ellipsoids are drawn at the 50% probability level. Hydrogen atoms (except in the anion) and solvent molecules have been omitted for clarity. Selected bond distances (Å) and angles (deg): Tl−Ctr(3) = 2.789, Tl−Ctr(4) = 2.855, Tl−C(31) = 3.150(3), Tl−C(32) = 3.109(3), Tl−C(33) = 3.122(3), Tl−C(34) = 3.111(3), Tl−C(35) = 3.116(3), Tl−C(36) = 3.136(3), Tl−C(41) = 3.185(4), Tl−C(42) = 3.197(4), Tl−C(43) = 3.199(4), Tl−C(44) = 3.171(4), Tl−C(45) = 3.153(4), Tl−C(46) = 3.154(4); Ctr(3)−Tl−Ctr(4) = 142.4.

distances to the bridging Tl atoms are noticeably longer than those to the terminal ones. The counteranions act as unsymmetrical bridging units between distinct $[Tl_4(\mu^3\text{-}OH)_2]^{2+}$ ions via C−F···Tl and C−F···H−O contacts; for example, O(1)−H(1)···F(5^E) shows a short distance of 2.30 Å. Each of the terminal thallium atoms Tl(2) and Tl(2^A) lies in a four-coordinate environment, since two F atoms of the neighboring counteranion and one Cl atom from a dichloromethane molecule can be considered as significantly coordinating [Tl(2)−F(8) = 3.143(3) Å, Tl(2)−F(29^D) = 3.025(3) Å and Tl(2)−Cl(1^D) = 3.269(2) Å; the van der Waals radii for Tl, F, and Cl are 2.00, 1.35, and 1.80 Å, respectively].[30,31] The two bridging Tl atoms are also four-coordinate, since the short Tl(1)···F(19^B) and Tl(1)···F(23^C) distances of 3.045(3) and 3.101(3) Å are indicative of strong interactions. The structure of the $[H_2N\{B(C_6F_5)_3\}_2]^-$ anion in **3** is very similar to that described for **2b**; four intramolecular N−H···F hydrogen bonds are found in the range 1.89−2.26 Å.

Although the solubility of **2a** in toluene at room temperature is limited, the compound dissolves on warming to 75 °C. The diethyl ether could be removed by bubbling dry argon through this solution at constant temperature for 150 min. Cooling gave a large quantity of oil which was isolated and washed repeatedly with light petroleum to yield a white powder. NMR spectra and microanalysis suggested the formation of $[Tl(toluene)_2][H_2N\{B(C_6F_5)_3\}_2]$ (**4a**) (Scheme 2). The ^1H and $^{13}C\{^1H\}$ NMR chemical shifts of the coordinated toluene molecules were extremely close to those of free toluene in the same deuterated solvent (CD_2Cl_2), which seemed to suggest weak coordination and ready dissociation of the arene ligands in solution. It has been reported previously that Tl(I)-arene complexes (arene = benzene,[6] mesitylene,[7−9,12] 1,2,4-trimethylbenzene[12,13]) readily lose the coordinated arenes upon heating and/or under vacuum. By contrast, heating **4a** to 70 °C under vacuum (0.01 mmHg) for 3 h provided no evidence for the loss of toluene; only prolonged exposure to higher temperatures (>80 °C) under vacuum resulted in the decomposition of the salt.

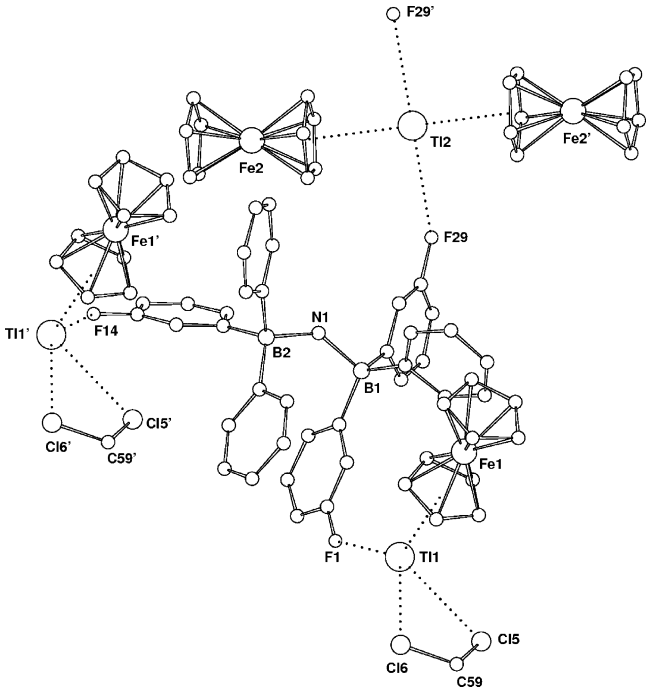

Figure 5. General view of the two cationic components $[Tl(FeCp_2)_2]^+$ and $[Tl(FeCp_2)]^+$ present in the crystal lattice, showing the contacts with a bridging $[H_2N\{B(C_6F_5)_3\}_2]^-$ counteranion. Each unit cell contains one linear $[Tl(FeCp_2)_2]^+$ cation, one $[Tl(FeCp_2)]^+$ cation and two anions. Nonbonding solvent molecules, hydrogen atoms and noninteracting fluorine atoms have been removed for clarity.

Recrystallization of a toluene solution of **4a** at −26 °C gave the tris(toluene) adduct $[Tl(toluene)_3][H_2N\{B(C_6F_5)_3\}_2]$ (**4b**) as colorless blocks. The solid-state structure was determined by X-ray diffraction (Figure 3). The environment around the thallium atom consists of three toluene rings, all of which are η^6-coordinated to the metal. To the best of our knowledge, **4b** constitutes the first example of a tris(toluene) adduct of thallium.

In the cation, the Tl(1)···C_{arene} distances to the carbon atoms of each of the three toluene molecules are in the ranges 3.273(5)−3.346(5), 3.158(4)−3.354(5) and 3.185(4)−3.316(5) Å, while the corresponding Tl···centroid distances Tl(1)···Ctr(1), Tl(1)···Ctr(2), and Tl(1)···Ctr(3) (Ctr = centroid) are 3.010, 2.947, and 2.942 Å, respectively. These values are indicative of very substantial interactions between the thallium atom and the coordinated arenes; they compare very well with the shortest distances reported for the other Tl(I)-(η^6-arene) complexes (Table 1).[7−14] For instance, Schmidbaur's $[Tl_4(mes)_6][GaBr_4]_4$[7] displays Tl···Ctr distances of 2.94 to 3.03 Å, while in Reed's $[Tl(toluene)_2][CB_{11}H_6Br_6]$,[14] the two toluene rings are located at a somewhat longer distance (Tl···Ctr = 2.99 and 3.09 Å).

(30) Pauling, L. *The Nature of the Chemical Bond*; Cornell University Press: Ithaca, NY, 1960; p 260.
(31) Bondi, A. *J. Phys. Chem.* **1964**, *68*, 441−451.

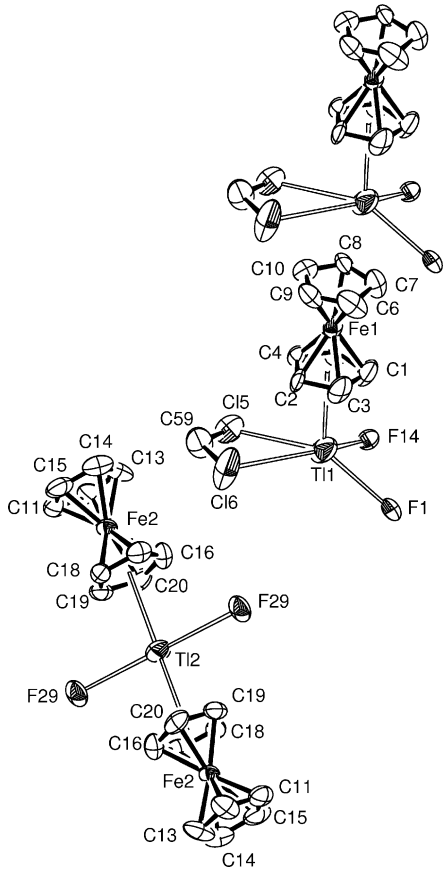

Figure 6. View of one $[Tl(FeCp_2)_2]^+$ and two $[Tl(FeCp_2)]^+$ ions in **6**, showing the significant interactions to the $[H_2N\{B(C_6F_5)_3\}_2]^-$ counteranions and to the solvent molecules, and indicating the numbering scheme. Thermal ellipsoids are drawn at the 50% probability level. Hydrogen atoms have been omitted for clarity. Selected bond distances (Å) and bond lengths (deg) in the $[Tl(FeCp_2)]^+$ cation: Tl(1)−Ctr(1a) = 2.923, Tl(1)−C(1) = 3.1059(3), Tl(1)−C(2) = 3.1386(3), Tl(1)−C(3) = 3.0687(3), Tl(1)−C(4) = 3.2634(3), Tl(1)−C(5) = 3.2015(3), Tl(1)−F(1) = 3.0277(3), Tl(1)−F(14) = 3.2655(3), Tl(1)−Cl(5) = 3.3387(3), Tl(1)−Cl(6) = 3.4422(3), Fe(1)−Ctr(1a) = 1.650, Fe(1)−Ctr(1b) = 1.676; Ctr(1b)−Fe(1)−Ctr(1a) = 178.56, Fe(1)−Ctr(1a)−Tl(1) = 174.87, Cl(5)−Tl(1)−Cl(6) = 50.90, Cl(5)−C(59)−Cl(6) = 114.8(13). Selected bond distances (Å) and bond lengths (deg) in the $[Tl(FeCp_2)_2]^+$ cation: Tl(2)−Ctr(2a) = 2.9309, Tl(2)−C(16) = 3.2849(3), Tl(2)−C(17) = 3.2152(3), Tl(2)−C(18) = 3.1006(3), Tl(2)−C(19) = 3.0526(3), Tl(2)−C(20) = 3.1761(3), Tl(2)−F(29) = 3.1833(3), Fe(2)−Ctr(2a) = 1.6484, Fe(2)−Ctr(2b) = 1.6378; Ctr(2b)−Fe(2)−Ctr(2a) = 178.17, Ctr(2a)−Tl(2)−Ctr(2a′) = 180, F(29)−Tl(2)−F(29′) = 180, F(29)−Tl(2)−Ctr(2a) = 91.75.

The sum of the Ctr(x)−Tl(1)−Ctr(x) angles is 359.7°, and the Tl atom lies only 0.088 Å out of the plane of the three centroids; the geometry about the Tl atom is essentially trigonal planar. Remarkably, in the solid state there is no interaction between the metal and the $[H_2N\{B(C_6F_5)_3\}_2]^-$ counteranion in **4b**. The shortest Tl(1)···F distance to the anion is 3.432(3) Å to F(27), that is, longer than the sum of the van der Waals radii for thallium (2.00 Å) and fluorine (1.35 Å).[30,31] This is unprecedented, as *all* other examples of Tl(I)−arene complexes, including those involving the weakly coordinating anion $[CB_{11}H_6Br_6]^-$,[14] feature some degree of anion coordination via Tl···X contacts (X = halogen,[7,9,11−14] hydrogen,[10] or oxygen[8,9]); in fact, in all cases but one,[10] the anion acts as a bridge between two or more cations (Table 1).

There are no thallium−thallium contacts in **4b**, as the two closest thallium atoms lie 9.429(3) Å apart. The structure of the anion in **4b** resembles very closely that of **2b**.

Scheme 3. Synthetic Routes for the Preparation of Thallium(I)−Chelating Ether Complexes

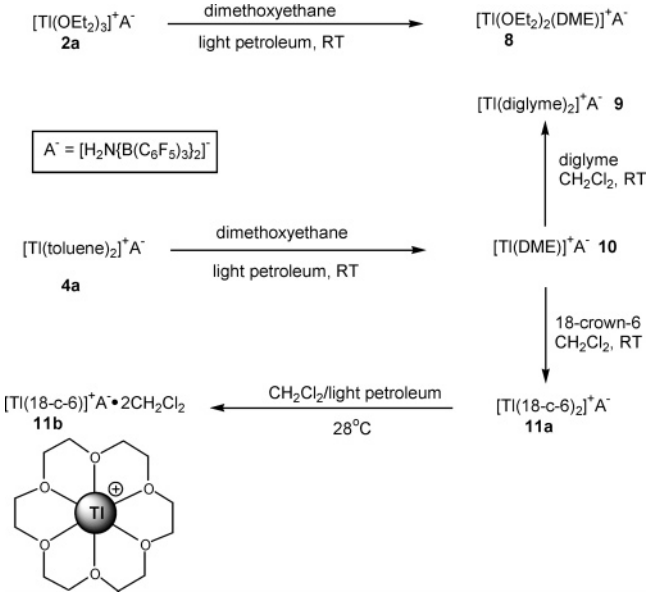

When dry argon was bubbled through a toluene solution of **2a** warmed to 75 ± 2 °C in presence of a large excess of hexamethylbenzene, the C_6Me_6 adduct $[Tl(C_6Me_6)_2][H_2N\{B(C_6F_5)_3\}_2]\cdot 1.5CH_2Cl_2$ (**5a**) was obtained in 74% yield (Scheme 2). Colorless crystals of $[Tl(C_6Me_6)_2][H_2N\{B(C_6F_5)_3\}_2]\cdot 2.5CH_2Cl_2$ (**5b**) were grown by recrystallization from a dichloromethane solution. The structure of **5b** was determined by X-ray diffraction crystallography. Previous attempts at isolating a thallium(I) hexamethylbenzene complex are reported to have failed,[7] and **5a**,**b** therefore represents the first examples of adducts between Tl(I) and this bulky arene. Complexes **5a** and **5b** are very soluble in chlorinated solvents, show moderate solubility in toluene, and are insoluble in light petroleum. The dichloromethane molecules could not be removed, even upon moderate heating under vacuum. There was no indication of significant interaction between the thallium atom and the counteranion in the ^{19}F NMR spectrum of **5a**.

Surprisingly, the arene exchange reaction has a significant activation barrier: heating a mixture of **4a** and C_6Me_6 in toluene to 60 °C instead of 75 °C under otherwise identical conditions failed to produce **5a**, and **4a** was recovered as the only product.

Single crystals of **5b** were obtained as colorless prisms. The structure of the salt is illustrated in Figure 4. The environment around the thallium ion consists only of two hexamethylbenzene molecules. There are 2.5 molecules of noncoordinated dichloromethane per thallium ion in the crystal lattice, and their positions were refined freely.

The two arene rings are η^6-coordinated to the heavy metal. The Tl···centroid distances of 2.789 and 2.855 Å are the shortest reported to date (Table 1); the corresponding $Tl\cdots C_{arene}$ distances are in the ranges 3.109(3)−3.150(3) and 3.153(4)−3.199(4) Å. These interactions are significantly stronger than, for instance, those found in **4b** or in $[(mes)_6Tl_4][GaBr_4]_4$[7] and $[Tl(mes)_2][B(OTeF_5)_4]$.[9] This is evidently accounted for by the fact that C_6Me_6 acts as a stronger donor toward the Tl^+ cation than other less electron-rich arenes such as mesitylene, toluene, or benzene and by the absence of anion coordination. The closest distances between Tl^+ and fluorine atoms F(22A), F(23A), F(13A), and

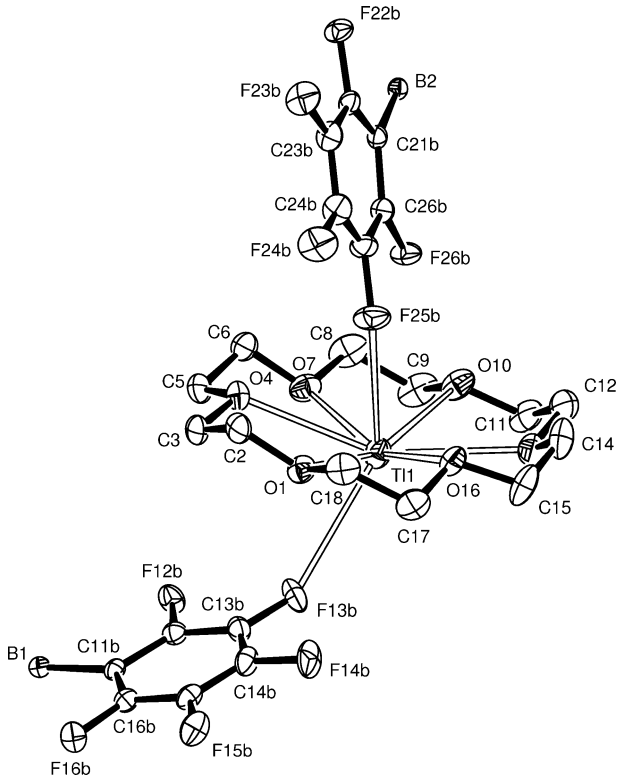

Figure 7. View of the cation in **11b** showing the significant Tl···F interactions to two counteranions. Hydrogen atoms have been omitted for clarity. Thermal ellipsoids are drawn at the 50% probability level. Selected bond distances (Å) and bond angles (deg): Tl(1)−O(1) = 2.879(2), Tl(1)−O(4) = 2.856(2), Tl(1)−O(7) = 2.855(2), Tl(1)−O(10) = 2.903(2), Tl(1)−O(13) = 2.875(2), Tl(1)−O(16) = 2.870(2), Tl(1)−F(13b′) = 3.111(2), Tl(1)−F(25b) = 3.105(2); O(4)−Tl(1)−O(1) = 58.58(6), O(7)−Tl(1)−O(1) = 118.11(7), O(7)−Tl(1)−O(4) = 59.73(7), O(1)−Tl(1)−F(13b′) = 62.97(6), O(1)−Tl(1)−F(25b) = 64.40(6), O(4)−Tl(1)−F(13b′) = 80.94(6), O(4)−Tl(1)−F(25b) = 66.04(6), O(7)−Tl(1)−F(13b′) = 103.22(6), O(7)−Tl(1)−F(25b) = 94.83(6), O(10)−Tl(1)−F(13b′) = 137.19(6), O(10)−Tl(1)−F(25b) = 94.99(6), O(13)−Tl(1)−F(13b′) = 121.32(6), O(13)−Tl(1)−F(25b) = 90.07(6), O(16)−Tl(1)−F(13b′) = 94.88(6), O(16)−Tl(1)−F(25b) = 63.52(6), F(25b)−Tl(1)−F(13b′) = 126.86(5).

F(12A) of the counteranion are 3.529(2), 3.535(2), 3.547(2), and 3.555(2) Å, respectively. That is at least 0.18 Å longer than the sum of the van der Waals radii of Tl and F (3.35 Å) and beyond bonding range.

The thallium sandwich has a bent geometry, with a Ctr(1)−Tl−Ctr(2) angle of 142.4°. This angle is much larger than the Ctr−Tl−Ctr angle of 111.8° found in $[Tl(toluene)_2][CB_{11}H_6Br_6]$;[14] the wider angle displayed in **5b** is obviously due to the lack of interaction between Tl^+ and the anion, whereas in $[Tl(toluene)_2][CB_{11}H_6Br_6]$ there are three additional Tl···Br contacts [3.421(2), 3.393(2), and 3.592(2) Å].

The facile formation of stable arene complexes suggested the possibility of generating thallium-bridged multidecker structures by coordinating Tl^+ to metallocenes. Thus the addition of ferrocene to a solution of **4a** in dichloromethane at room temperature (Scheme 2) gave a product of the composition $[Tl_2(FeCp_2)_3][H_2N\{B(C_6F_5)_3\}_2]_2\cdot 5CH_2Cl_2$ (**6**) in high yield. The ^1H and $^{13}C\{^1H\}$ NMR spectra showed only one set of resonances for all C_5H_5 rings, while the ^{11}B and ^{19}F NMR spectra very closely resembled those of **4a** and **5a**. Compound **6** is highly soluble in chlorinated solvents but insoluble in light petroleum.

Crystals suitable for X-ray diffraction were isolated as light-orange plates by cooling a concentrated dichloromethane solution to −28 °C. The structure of **6** (Figure 5) shows the presence of two different complex cations, $[Tl(FeCp_2)]^+$ and $[Tl(FeCp_2)_2]^+$, in a 1:1 ratio. It consists of the cations $[Tl(FeCp_2)_2]^+$ and $[Tl(FeCp_2)]^+$, with sandwich and half-sandwich structures, respectively, paired with $[H_2N\{B(C_6F_5)_3\}_2]^-$ anions. To the best of our knowledge, there is no literature precedent for thallium-based heterobimetallic complexes assembled through Tl(I)−arene interactions.

The anion acts as an unsymmetrical bridging ligand between the two different types of cations via Tl···F contacts. In addition, the unit cell also contains five molecules of dichloromethane which have been refined freely. One of these solvent molecules is coordinated to Tl(1), the thallium ion which carries the single ferrocene ligand. The remaining four CH_2Cl_2 molecules do not interact with the cations. The thallium atom Tl(2) lies at a center of inversion.

The structures of the two distinct cations are illustrated in Figure 6. In the $[Tl(FeCp_2)_2]^+$ fragment, the environment around Tl(2) consists of two η^5-coordinated aromatic rings and two relatively close fluorine atoms. The two ferrocene ligands built around Fe(2) and Fe(2′) are symmetrically related by inversion at Tl(2). The Tl(2)−C_{ring} distances to C(16), C(17), C(18), C(19), and C(20) are, respectively, 3.2849(3), 3.2152(3), 3.1006(3), 3.0526(3), and 3.1761(3) Å. The corresponding Tl−Ctr(2a) distance of 2.9309 Å (Ctr = centroid) compares well with those found in **4b** or other known examples but is noticeably longer than that found in the hexamethylbenzene complex **5b**

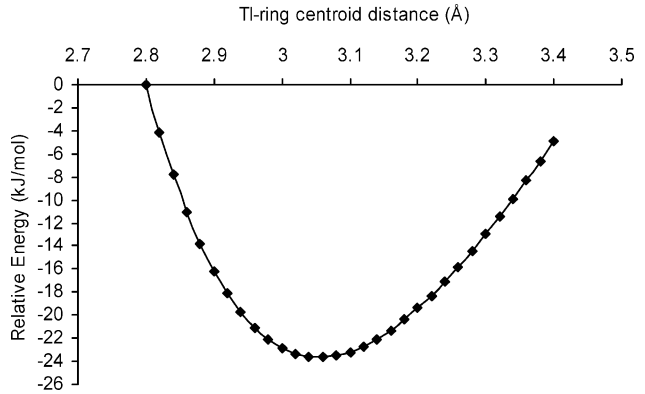

Figure 8. Plot of Tl−benzene interaction energy versus Tl···Ctr distance for $[Tl(benzene)_3]^+$; for each point the Tl···Ctr distances are fixed but all other parameters are allowed to optimize. The energy of the molecule was arbitrarily set to 0 kJ/mol for Tl···Ctr = 2.8 Å.

Scheme 4. Synthetic Pathways for the Preparation of Thallium(I)−Chelating Arenes Complexes

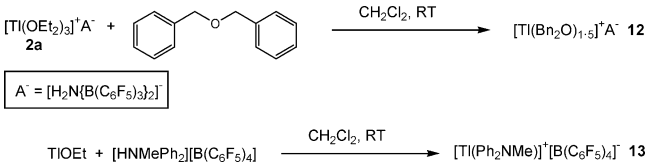

Scheme 5. ^{205}Tl NMR Chemical Shifts for Compounds **2a**, **4a**, **5a**, **12**, and **13** in CD_2Cl_2

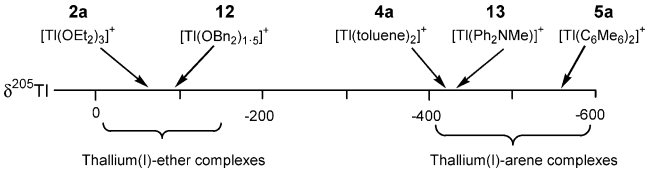

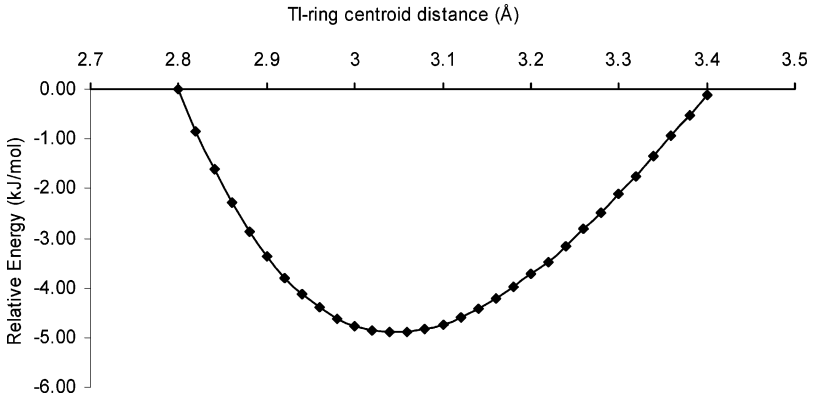

Figure 9. Plot of Tl−benzene interaction energy versus Tl···Ctr distance for $[Tl(benzene)_3]^+$; two of the benzene rings are fixed at their positions in the optimized structure and the Tl···Ctr distance for the third ring is allowed to optimize (all other parameters in ring 3 being free to optimize). The energy of the molecule was arbitrarily set to 0 kJ/mol for Tl···Ctr = 2.8 Å.

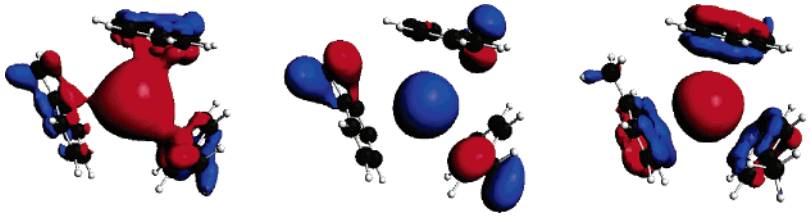

Figure 10. Valence molecular orbitals with Tl s character in $[Tl(tol)_3]^+$: (left) bonding between the Tl and the in-phase combination of the toluene π_1 orbitals; (center) thallium−toluene nonbonding; (right) antibonding between Tl and the in-phase combination of the toluene π_1 orbitals.

(Table 1). The two fluorine atoms F(29) and F(29′) are also symmetry-related and can be considered as weakly interacting with the thallium atom on account of the Tl(2)−F(29) distance of 3.1833(3) Å, slightly shorter than the sum of the van der Waals radii (3.35 Å). If one considers the two centroids Ctr(2a) and Ctr(2a′) and the two fluorine atoms F(29) and F(29′), the geometry around Tl(2) is very close to square planar. The coordination of the cyclopentadienyl ring C(16−20) [corresponding centroid Ctr(2a)] to the thallium atom Tl(2) has little influence on the geometry of the whole ferrocene moiety, as indicated by the almost identical bond lengths Fe(2)−Ctr(2a) and Fe(2)−Ctr(2b) [1.6484 and 1.6378 Å] and the Ctr(2b)−Fe(2)−Ctr(2a) angle of 178.17°.

In the $[Tl(FeCp_2)]^+$ fragment, the Tl(1)−Ctr(1a) distance of 2.923 Å to the centroid of the η^5-C_5H_5 ring is very close to that found in $[Tl(FeCp_2)_2]^+$. The geometry of the ferrocene around Fe(1) is only marginally perturbed by the coordination to the thallium atom Tl(1) [Fe(1)−Ctr(1a) = 1.650 Å, Fe(1)−Ctr(1b) = 1.676 Å; Ctr(1b)−Fe(1)−Ctr(1a) = 178.56°], and the Fe(1)−Ctr(1a)−Tl(1) arrangement is almost linear (angle 174.87°). The environment around Tl(1) is completed by two fluorine and two chlorine atoms. The interaction with F(1) is substantial, Tl(1)−F(1) = 3.0277(3) Å, and clearly stronger than that with F(14) (3.2655(3) Å), while there is also some asymmetry in the contact distances to Cl(5) (3.3387(3) Å) and Cl(6) (3.4422(3) Å). The Cl(5)−Tl(1)−Cl(6) angle of 50.90° is very acute, whereas the Cl(5)−C(59)−Cl(6) angle (114.8(13)°) is in the normal range. The $[Tl(FeCp_2)]^+$ units are repeated by translation in columns along the *a*-axis and roughly along the Tl(1)···Fe(1) direction (Figure 6). However, these columns are disordered, either as shown running down the page or in the inverted orientation (related by a center of symmetry close to C(9)) running up the page.

In contrast to the formation of ferrocene adducts, the addition of decamethylferrocene $FeCp^*_2$ to a dichloromethane solution

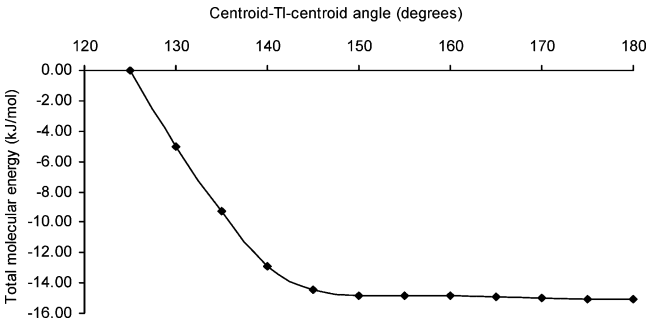

Figure 11. Total molecular energy in $[Tl(C_6Me_6)_2]^+$ as a function of the Ctr(3)−Tl−Ctr(4) angle. The energy of the molecule was arbitrarily set to 0 kJ/mol for ∠Ctr(3)−Tl−Ctr(4) = 125 °.

of **4a** leads to an immediate redox reaction, to give thallium metal together with dark-green $[FeCp^*_2][H_2N\{B(C_6F_5)_3\}_2]\cdot CH_2Cl_2$ (**7**, for crystallographic characterization see Supporting Information). Presumably, this electron-transfer reaction is preceded by the formation of a thallium−metallocene adduct akin to complex **6**. It is tempting therefore to consider the ferrocene adduct **6** as a model close to the transition state in the redox process.

The thallium ether and arene complexes are convenient starting materials for ligand exchange reactions. Thus complex **4a** readily reacts with $(C_5Me_5)SnCl$ in dichloromethane under halide exchange to give $[(C_5Me_5)Sn][H_2N\{B(C_6F_5)_3\}_2]\cdot 1.5CH_2Cl_2$ in high yield (see Supporting Information). Compounds **2a** and **4a** were also reacted with various chelating ethers in order to explore briefly the coordination chemistry of Tl(I) salts (Scheme 3). For example, the addition of an excess of dimethoxyethane (DME) to a suspension on **2a** in light petroleum gave the three-coordinate $[Tl(DME)(Et_2O)][H_2N\{B(C_6F_5)_3\}_2]$ (**8**) in high yield. The two toluene molecules on the thallium atom are easily displaced by the chelate in the

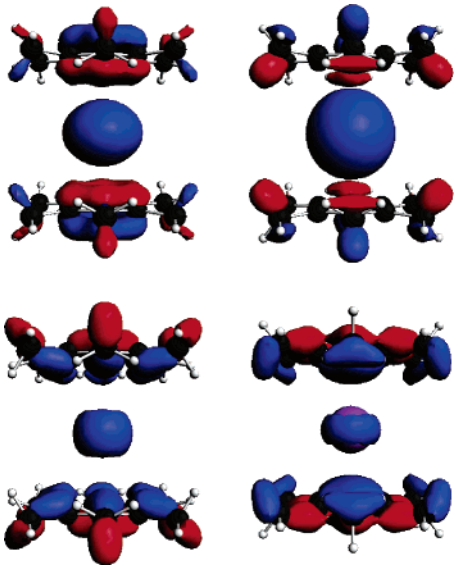

Figure 12. Valence molecular orbitals with Tl s character in $[Tl(C_6Me_6)_2]^+$ at ∠Ctr(3)−Tl−Ctr(4) = 180 °: $25a_1$, top left; $21a_1$, top right; $15a_1$, bottom left; $14a_1$ (the most stable), bottom right.

reaction of **4a** with DME in light petroleum, resulting in the quantitative formation of the 1:1 adduct $[Tl(DME)][H_2N\{B(C_6F_5)_3\}_2]$ (**9**). The six-coordinate $[Tl(diglyme)_2][H_2N\{B(C_6F_5)_3\}_2]$ (**10**) was prepared in 90% yield by further reaction of **9** with diethylene glycol dimethyl ether (diglyme). Although **8**−**10** were fully characterized by ^1H, $^{13}C\{^1H\}$, ^{11}B, and ^{19}F NMR spectroscopy and elemental analysis, structural information is not available as stable single crystals suitable for X-ray diffraction studies could not be isolated.

On the addition of 18-crown-6 to a solution of **9** in dichloromethane, the 1:2 complex $[Tl(18\text{-crown-}6)_2][H_2N\{B(C_6F_5)_3\}_2]$ (**11a**) was isolated as a white solid. The composition of this compound was confirmed by NMR spectroscopy and microanalysis. On recrystallization from a CH_2Cl_2/light petroleum mixture, however, single crystals of the 1:1 adduct $[Tl(18\text{-crown-}6)][H_2N\{B(C_6F_5)_3\}_2]\cdot 2CH_2Cl_2$ (**11b**) were isolated; the structure was determined by X-ray diffraction. On drying in vacuo, this compound lost the solvent molecules to give $[Tl(18\text{-crown-}6)][H_2N\{B(C_6F_5)_3\}_2]$ (**11c**).

In the crystal the thallium cation in **11b** (Figure 7) is eight-coordinate. Related structures have been described.[32−35] The thallium atom Tl(1) is bonded to all six crown-ether O atoms and is positioned slightly out of the plane formed by the six oxygen atoms. The Tl(1)−O distances are in the range 2.855(2)−2.903(2) Å and are slightly smaller than those found in $[\{Tl(18\text{-crown-}6)\}_4MnCl_4][TlCl_4]_2$ (2.93−3.01 Å)[33] and [Tl(18-crown-6)(OC_6F_5)] (average 2.97 Å).[35] The coordination sphere is completed by two Tl···F interactions, Tl(1)−F(25B) and Tl(1)−F(13B′), at distances of 3.105(2) and 3.111(2) Å, respectively. The two CH_2Cl_2 molecules are disordered and show no interactions with the cation. It is interesting to note that complex **11b**, where the coordination sphere would be expected to be saturated by the six crown-ether oxygen donors, shows significant anion binding, whereas complexes **4** and **5**, with their weaker and more labile arene ligands, do not, a clear indication that the coordination to Tl(I) is dictated primarily by steric and electrostatic factors.

With the aim of preparing a thallium(I)-chelating arene complex, **2a** was reacted with an excess of dibenzyl ether (OBn_2) in dichloromethane (Scheme 4), to yield $[Tl(Bn_2O)_{1.5}][H_2N\{B(C_6F_5)_3\}_2]$ (**12**). Similarly, the protolysis of thallium ethoxide with $[Ph_2MeNH][B(C_6F_5)_4]$ in dichloromethane neatly afforded $[Tl(Ph_2MeN)][B(C_6F_5)_4]$ (**13**) in 80% yield. The ^1H and $^{13}C\{^1H\}$ NMR spectra of **12** and **13** gave no information regarding the coordination mode of the potentially chelating OBn_2 and $MeNPh_2$ ligands, and repeated attempts to grow crystals proved unsuccessful. However, use of ^{205}Tl NMR spectroscopy allowed us to establish the coordination modes of these heteroatom-containing ligands (see later).

Solution ^{205}Tl NMR Spectroscopy. The ^{205}Tl isotope has an abundance of 70.5%, its sensitivity is more than 300 times greater that that of ^{13}C, and it has a very wide chemical-shift range which is very sensitive to the coordination environment. The ^{205}Tl NMR spectra of **2a**, **4a**, **5a**, **12**, and **13** were recorded in deuterated dichloromethane and externally referenced to $TlNO_3$ in D_2O. Because of the high molecular weights of these compounds, the metal loading for each sample was very limited. For each complex, the spectrum revealed a single, rather broad resonance (line width 700−5000 Hz; see Supporting Information).

The compounds fall into two distinctive classes based on their chemical shifts. The diethyl ether complex **2a** gives rise to a very broad signal centered on δ −53. By contrast, the signals for the two thallium arene complexes **4a** and **5a** are comparatively narrow and are centered on δ −425 and −563, respectively, that is, there is a considerable shift toward high fields with respect to **2a**.

The ^{205}Tl NMR spectrum of **12** exhibits a relatively sharp signal at δ −99 ppm, very close to that found for **2a**, which suggests that OBn_2 coordinates to thallium via its oxygen atom and not via the arene rings. On the other hand, the broader resonance for **13** is located at δ −435 and is almost identical to that found for the bis(toluene) adduct **4a**, which suggests that unlike OBn_2, $NMePh_2$ coordinates via its arene rings (Scheme 5). These observations agree with previously reported ^{205}Tl chemical shifts for thallium complexes of crown ethers[36−38] and calixarenes.[39]

DFT Calculations. In order to gauge the strength of the interactions between the thallium atom and the arene rings in **4b** and **5b** and to get a better understanding of the structures of these two compounds, density-functional theory (DFT) calculations were carried out using the Amsterdam density functional (ADF) program suite (see Experimental Section).[40−45]

(32) Kahwa, I. A.; Miller, D.; Mitchell, M.; Fronczek, F. R. *Acta Crystallogr., Sect. C: Cryst. Struct. Commun.* **1993**, *49*, 320−321.
(33) Fender, N. S.; Finegan, S. S.; Miller, D.; Mitchell, M.; Kahwa, I. A.; Fronczek, F. R. *Inorg. Chem.* **1994**, *33*, 4002−4008.
(34) Mudring, A;-V.; Rieger, F. *Inorg. Chem.* **2005**, *44*, 6240−6243.
(35) Childress, M. V.; Millar, D.; Alam, T. M.; Kreisel, K. A.; Yap, G. P. A.; Zakharov, L. N.; Golen, J. A.; Rheingold, A. L.; Doerrer, L. H. *Inorg. Chem.* **2006**, *45*, 3864−3877.
(36) Srivanavit, C.; Zink, J. I.; Dechter, J. J. *J. Am. Chem. Soc.* **1977**, *99*, 5876−5881.
(37) Gudlin, D.; Schneider, H. *Inorg. Chim. Acta* **1979**, *33*, 205−208.
(38) Shamsipur, M.; Popov, A. I. *Inorg. Chim. Acta* **1980**, *43*, 243−247.
(39) Matthews, S. E.; Rees, N. H.; Felix, V.; Drew, M. G. B.; Beer, P. D. *Inorg. Chem.* **2003**, *42*, 729−734.
(40) Constantine, S. P.; De Lima, G. M.; Hitchcock, P. B.; Keates, J. M.; Lawless, G. A.; Marziano, I. *Organometallics* **1997**, *16*, 793−795.
(41) *ADF2000*; Department of Theoretical Chemistry, Vrije Universiteit: Amsterdam, The Netherlands, 2000.
(42) Baerends, E. J.; Ellis, D. E.; Ros, P. *Chem. Phys.* **1973**, *2*, 41−51.
(43) Versluis, L.; Ziegler, T. *J. Chem. Phys.* **1988**, *88*, 322−328.

Table 2. Crystal and Structure Refinement Data for Compounds **2b**, **3**, and **4b**

	2b	3	4b
elemental formula	$C_{16}H_{40}O_4Tl$, $C_{36}H_2B_2F_{30}N$	$H_2O_2Tl_4$, 2($C_{36}H_2$ $B_2F_{30}N$), 4(CH_2Cl_2)	$C_{21}H_{24}Tl$, $C_{36}H_2B_2F_{30}N$
fw	1540.9	3271.2	1520.8
cryst syst	triclinic	triclinic	monoclinic
space group	$P\bar{1}$ (No. 2)	$P\bar{1}$ (No. 2)	$P2_1/c$ (No. 14)
unit cell dimensions			
a (Å)	12.2481(4)	11.4827(11)	13.781(5)
b (Å)	13.7603(5)	14.1996(12)	18.151(8)
c (Å)	17.3040(6)	14.2725(8)	21.698(14)
α (deg)	86.556(2)	105.075(5)	90
β (deg)	76.904(2)	92.968(9)	91.68(5)
γ (deg)	87.120(2)	101.382(7)	90
cell volume, V (Å^3)	2833.38(17)	2189.7(3)	5425(5)
no. of formula units/cell, Z	2	1	4
density (calcd) (Mg/m^3)	1.806	2.481	1.862
F(000)	1508	1520	2944
abs coeff (mm^{-1})	2.995	7.760	3.123
T (K)	120(2)	120(2)	120(2)
cryst color, shape	colorless block	colorless block	colorless block
cryst size (mm)	0.36 × 0.2 × 0.2	0.28 × 0.10 × 0.10	0.06 × 0.06 × 0.06
on the diffractometer:			
θ range for data collection	2.9−27.2°	3.0−27.5°	3.6−27.5°
index ranges for h, k, l	−15/15, −17/17, −22/22	−14/14, −18/18, −18/18	−17/17, −23/23, −28/28
max and min transm	1.00, 0.64	0.51, 0.22	1.00, 0.75
total no. of reflctns measd	56483	53697	91366
no. of unique reflctns	12419	10044	12426
r_{int} for equivalents	0.058	0.036	0.067
no. of obsd reflctns ($I > 2\sigma_I$)	8937	9127	9689
refinement:			
data/restraints/params	12419/0/850	10044/0/703	12426/0/823
GOF on F^2, S	1.064	1.092	1.082
final R indices (obsd data)	$R_1 = 0.048$	$R_1 = 0.034$	$R_1 = 0.048$
	$wR_2 = 0.106$	$wR_2 = 0.082$	$wR_2 = 0.075$
final R indices (all data)	$R_1 = 0.080$	$R_1 = 0.039$	$R_1 = 0.071$
	$wR_2 = 0.113$	$wR_2 = 0.084$	$wR_2 = 0.081$
reflctns weighted:[a] (A, B)	0.0378, 5.94	0.0298, 9.54	0.0111, 12.53
largest diff. peak and hole (e.Å^{-3})	0.83 and −0.95	1.71 and −2.42	1.09 and −1.14

[a] Weighting scheme applied: $w = [\sigma^2(F_o^2) + (AP)^2 + BP]^{-1}$, where $P = (F_o^2 + 2F_c^2)/3$.

The interaction of the Tl atom with the three toluene rings in **4b** was investigated by calculating the interaction energy for the simplified model $[Tl(benzene)_3]^+$. An initial series of restricted geometry optimizations was performed in which at each point the Tl···Ctr (Ctr = centroid) distances were fixed but all other parameters are allowed to optimize; the results obtained when the three rings are moved simultaneously are shown in Figure 8. The overall stabilization is 23.5 kJ mol^{-1} and the corresponding minimum Tl···Ctr distance of 3.06 Å is in good agreement with the structural parameters found in **4b** (Tl···Ctr = 2.94, 2.95, and 3.01 Å). A second series of calculations were performed in which two of the rings were fixed at their positions in the optimized structure and the Tl···Ctr distance for the third ring varied (all other parameters in ring 3 being free to optimize within the constraint of D_{3h} symmetry). The energy well resulting from this process is extremely shallow (Figure 9); the minimum Tl···Ctr distance of 3.06 Å corresponds to a stabilization of only 4.9 kJ mol^{-1}.

Next, the geometry of $[Tl(tol)_3]^+$ was optimized, and converged to a structure very similar to that obtained experimentally, and indeed to that calculated for $[Tl(benzene)_3]^+$. The Mulliken charge for Tl in $[Tl(tol)_3]^+$ at this geometry is +0.90, while the carbon atoms all have small negative charges and the hydrogens have small positive charges. The Tl charge is remarkably close to the formal oxidation state and indicates that the overall charge of **4b** is very much localized on the metal atom.

The interaction energy between the three toluene ligands and the Tl^+ ion in **4b** was computed using the fragment-based approach in ADF and is 221 kJ mol^{-1}. By contrast, the interaction energy of three toluene rings and a neutral Tl atom, calculated for $Tl(tol)_3$ at the optimized geometry of $[Tl(tol)_3]^+$, is only 51 kJ mol^{-1}. Thus, the bulk of the metal−ring interaction energy appears to be ionic (polarization/attraction). To probe this further, the molecular orbital (MO) structure of the cation was examined. The first six HOMOs are combinations of the ligand π_2 orbitals (i.e., the π orbitals of toluene with a single vertical node). Each of these orbitals is more than 95% ring-π in character, with essentially no contribution from the metal. In fact, virtually all the valence MOs are localized on the toluene rings, with the exception of three orbitals with thallium-s character. The lowest of these is bonding between Tl and an in-phase combination of the toluene π_1 orbitals (those with no vertical nodes). The middle one is metal-ring nonbonding, while the least stable (the seventh HOMO) is antibonding between the Tl and the in-phase combination of the toluene π_1 orbitals. These three orbitals are shown in Figure 10. Overall, therefore, there is very little evidence of covalency in **4b**, and what there is can have essentially no net effect as both bonding and antibonding combinations are filled.

(44) te Velde, G.; Baerends, E. J. *J. Comp. Phys.* **1992**, *99*, 84−98.
(45) Fonseca Guerra, C.; Snijders, J. G.; te Velde, G.; Baerends, E. J. *Theor. Chem. Acc.* **1998**, *99*, 391−403.

Table 3. Crystal and Structure Refinement Data for Compounds **5b**, **6** and **11b**

	5b	6	11b
elemental formula	$C_{24}H_{36}Tl$ $C_{36}H_2B_2F_{30}N$ 2.5(CH_2Cl_2)	$C_{10}H_{10}FeTl$ $C_{20}H_{20}Fe_2Tl$ 2($C_{36}H_2B_2F_{30}N$) 5(CH_2Cl_2)	$C_{12}H_{24}O_6Tl$ $C_{36}H_2B_2F_{30}N$ 2(CH_2Cl_2)
fw	1781.2	3471.5	1678.5
cryst syst	triclinic	triclinic	triclinic
space group	$P\bar{1}$ (No. 2)	$P\bar{1}$ (No. 2)	$P\bar{1}$ (No. 2)
unit cell dimensions			
a (Å)	12.2427(5)	10.0625(9)	12.4566(3)
b (Å)	13.9012(4)	11.6162(10)	15.7031(6)
c (Å)	19.1784(6)	24.6374(19)	16.4745(10)
α (deg)	84.244(2)	82.719(7)	73.710(4)
β (deg)	86.754(3)	81.749(7)	87.071(4)
γ (deg)	87.660(3)	84.366(7)	72.249(3)
cell volume, *V* (Å^3)	3240.24(19)	2817.6(4)	2943.8(2)
no. of formula units/cell, *Z*	2	1	2
density (calcd) (Mg/m^3)	1.826	2.046	1.894
F(000)	1742	1670	1628
abs coeff (mm^{-1})	2.828	3.615	3.069
T (K)	140(1)	140(1)	140(1)
cryst color, shape	colorless prism	light orange plate	colorless block
cryst size (mm^3)	0.45 × 0.30 × 0.20	0.50 × 0.25 × 0.04	0.68 × 0.35 × 0.26
on the diffractometer:			
θ range for data collection	3.5−25.0°	3.7−29.8°	3.6−27.5°
index ranges for *h*, *k*, *l*	−14/14, −16/16, −22/22	−13/14, −15/16, −34/34	−16/16, −20/20, −21/21
max and min transm	1.049 and 0.960	0.87, 0.42	1.138, 0.860
total no. of reflctns measd	35169	38083	42459
no. of unique reflctns	11290	14076	13363
r_{int} for equivalents	0.047	0.058	0.029
no. of obsd reflctns ($I > 2\sigma_I$)	9319	6527	11222
refinement:			
data/restraints/params	11290/0/949	14076/6/916	13363/0/884
GOF on F^2, *S*	1.011	0.946	1.052
final *R* indices (obsd data)	$R_1 = 0.032$ $wR_2 = 0.073$	$R_1 = 0.067$ $wR_2 = 0.159$	$R_1 = 0.030$ $wR_2 = 0.080$
final *R* indices (all data)	$R_1 = 0.043$ $wR_2 = 0.075$	$R_1 = 0.151$ $wR_2 = 0.177$	$R_1 = 0.039$ $wR_2 = 0.083$
reflctns weighted:[a] (*A*, *B*)	0.0429, 0	0.0888, 0	0.0509, 1.27
largest diff. peak and hole (e.Å^{-3})	2.36 and −1.54	1.29 and −1.01	1.17 and −1.17

[a] Weighting scheme applied: $w = [\sigma^2(F_o^2) + (AP)^2 + BP]^{-1}$, where $P = (F_o^2 + 2F_c^2)/3$.

The calculated interaction energy in $[Tl(C_6Me_6)_2]^+$ was found to be 243.4 kJ mol^{-1}. This corresponds to a Tl−C_6Me_6 bond energy of 121.7 kJ mol^{-1}, compared to 73.7 kJ mol^{-1} for toluene. The bond to the more electron rich arene is therefore considerably stronger, in line with the observed shorter Tl−Ctr(C_6Me_6) distances.

Calculations on $[Tl(C_6Me_6)_2]^+$ (**5b**) to establish whether a linear or bent geometry is the most stable revealed a very flat potential-energy surface for distortions of the Ctr(3)−Tl−Ctr(4) angle (Figure 11).

The change in the total bonding energy of the molecule between 145 and 180° is less than 1 kJ mol^{-1}. As the angle becomes smaller, the energy decreases (i.e., the molecule becomes less stable), presumably because the rings begin to interact unfavorably with each other. Overall, however, there is very little energetic preference for one particular geometry over another above about 140°. This is in good agreement with the crystallographic geometry [Ctr(3)−Tl−Ctr(4) 142.4°].

The structure of $[Tl(C_6Me_6)_2]^+$ may, as suggested by a reviewer, be compared with that of the anion in $[CpMg(PMDETA)]^+$ $[TlCp_2]^-$, which shows a somewhat wider Ctr−Tl−Ctr angle of 156.7°.[46] In view of the very flat energy profile shown above these angles, this would appear to be dictated primarily by packing forces.

Figure 11 implies that there is little or no directionality to the metal-ring bonding. To probe this, the electronic structure of $[Tl(C_6Me_6)_2]^+$ was calculated at the most stable geometry (180°). The computed Mulliken charge on the Tl is +0.91, essentially the same as in $[Tl(tol)_3]^+$, very much suggesting a Tl^+ ion sandwiched between two neutral rings. The MO structure is consistent with this for, as with $[Tl(tol)_3]^+$, there are very few valence MOs with any significant Tl character. Those that feature a Tl contribution do not show much evidence of metal-ring covalency (Figure 12). They all are of a_1 symmetry (in C_{2v}), with a Tl s contribution. All are nondirectional in terms of metal-ring bonding.

To investigate the reasons for the variations in the number of coordinated arene molecules between $[Tl(tol)_3]^+$ (in **4b**) and $[Tl(C_6Me_6)_2]^+$ (in **5b**), the geometries of $[Tl(tol)_2]^+$ and $[Tl(C_6Me_6)_3]^+$ have been optimized. $Tl(tol)_2^+$ plus an isolated toluene ligand is calculated to be 50 kJ mol^{-1} less stable than $[Tl(tol)_3]^+$. On the other hand, $[Tl(C_6Me_6)_2]^+$ plus an isolated C_6Me_6 ligand is only 28 kJ mol^{-1} less stable than $[Tl(C_6Me_6)_3]^+$. Hence, it is favorable for both systems to coordinate three arene rings but less so for the bulkier C_6Me_6 system; it is therefore probable that compound **5b** was isolated after the loss of a

(46) Armstrong, D. R.; Herbst-Irmer, R.; Kuhn, A.; Moncrieff, D.; Paver, M. A.; Russell, C. A.; Stalke, D.; Steiner, A.; Wright, D. S. *Angew. Chem., Int. Ed. Engl.* **1993**, *32*, 1774−1776.

loosely bound C_6Me_6 ring from the more thermodynamically stable initial product $[Tl(C_6Me_6)_3][H_2N\{B(C_6F_5)_3\}_2]$.

The various potential surfaces calculated above for $[Tl(tol)_3]^+$ and $[Tl(C_6Me_6)_2]^+$ are all very flat, and the energy discrepancies for different arrangements of the arene rings are very small. Moreover, these cations seem very much dominated by polarization bonding, with little or no directionality. This suggests that observations such as one of the three toluene molecules in **4b** being asymmetrically coordinated or the bent geometry of the cation in **5b** are unlikely to have an intramolecular explanation but, instead, that distortions are most probably the result of intermolecular interactions, perhaps from oft-mentioned crystal packing forces.

Conclusions

Weakly coordinating perfluoroaryl borate anions allow the characterization of thallium(I) salts with labile ligands and have provided the first structurally characterized examples of thallium diethyl ether and hexamethylbenzene complexes. In particular, the complex cations $[Tl(toluene)_3]^+$, $[Tl(C_6Me_6)_2]^+$, and $[Tl(Et_2O)_4]^+$ show no close contact to the anion. By contrast, the rather flat coordination geometry of crown ethers allows an increase in coordination number, with additional Tl···F contacts in axial positions, an indication of the importance of electrostatic effects on the coordination geometry of thallium. The bonding in the arene complexes was explored by DFT calculations and found to be predominantly due to polarization effects, without geometric preferences other than those provided by ligand repulsion. Whereas the readily reduced decamethylferrocene undergoes redox reactions with Tl(I), ferrocene itself forms stable multidecker adducts of the type $[Tl-Fc]^+$ and $[Fc-Tl-Fc]^+$ which may be regarded as models for the π-complex formed en-route to the electron-transfer step.

Experimental Section

General Procedures. All manipulations were performed under argon using standard Schlenk techniques with flame-dried glassware. Solvents were predried, and distilled under inert atmosphere over sodium (low-sulfur toluene), sodium-benzophenone ketyl (diethyl ether, THF), sodium-potassium alloy (light petroleum, boiling point 40−60 °C), or calcium hydride (dichloromethane). NMR solvents were dried over activated 4 Å molecular sieves and degassed by several freeze−thaw cycles. ^1H, $^{13}C\{^1H\}$, ^{11}B, ^{19}F, and ^{119}Sn NMR spectra were recorded using a Bruker DPX300 spectrometer. ^1H NMR spectra (300.13 MHz) are referenced to the residual protons of the deuterated solvent used. ^{13}C NMR spectra (75.47 MHz) were referenced internally to the D-coupled ^{13}C resonances of the NMR solvent. ^{11}B (96.29 MHz), ^{19}F (282.38 MHz), and ^{119}Sn (111.91 MHz) NMR spectra were referenced externally to $BF_3{\cdot}Et_2O$, $CFCl_3$, and $SnMe_4$, respectively. ^{205}Tl NMR spectra (288.49 MHz) were recorded on a Bruker DPX500 spectrometer equipped with a SEX $^{19}F/^{205}Tl$ probe head and were referenced with a 0.1 M solution of $TlNO_3$ in D_2O. Chemical shifts are reported in ppm, and all coupling constants are reported in Hertz. The infrared spectra (Nujol) were obtained using a Perkin-Elmer Spectrum 1000 FT-IR spectrometer. Thallium ethoxide, diphenylmethylamine, ferrocene, decamethylferrocene, and 18-crown-6 were used as purchased without further purification. Hexamethylbenzene was sublimed under vacuum (10^{-3} Torr). Dibenzyl ether, diethylene glycol dimethyl ether (diglyme), and 1,2-dimethoxyethane were dried over sodium and distilled prior to use. Compounds $[H(OEt_2)_2][H_2N\{B(C_6F_5)_3\}_2]$ (**1**)[1] and $[Ph_2MeNH][B(C_6F_5)_4]$[47] were prepared according to literature methods. CAUTION: Thallium compounds are toxic. Care must be taken when manipulating TlOEt.

Synthesis of $[Tl(OEt_2)_n][H_2N\{B(C_6F_5)_3\}_2]$ (2a, $n = 3$; 2b, $n = 4$). The addition of **1** (8.00 g, 6.7 mmol) to a solution of TlOEt (1.75 g, 7.0 mmol) in diethyl ether (50 mL) gave a colorless solution which was stirred overnight. The removal of volatiles under vacuum yielded a sticky foam which was washed repeatedly with light petroleum (5 × 50 mL) to give a fine white powder, yield 6.88 g (70%). NMR spectra and elemental analyses performed at this stage were consistent with the formulation $[Tl(OEt_2)_3][H_2N\{B(C_6F_5)_3\}_2]$ (**2a**). Anal. Calcd for $C_{48}H_{32}B_2F_{30}NO_3Tl$ (%): C, 39.31; H, 2.20; N, 0.95. Found: C, 39.42; H, 2.32; N, 0.98. ^1H NMR (CD_2Cl_2, 25 °C, 300.13 MHz): δ 5.72 (br s, 2H, NH_2), 3.60 (q, 12H, $J = 7.01$ Hz, CH_2−O), 1.27 (t, 18H, $J = 7.01$ Hz, CH_3) ppm. $^{13}C\{^1H\}$ NMR (CD_2Cl_2, 25 °C, 75.47 MHz): δ 149.7, 146.6, 141.1, 138.7, 137.8, 135.6 (all Ar−C_6F_5), 66.1 (CH_2−O), 15.3 (CH_3) ppm. ^{11}B NMR (CD_2Cl_2, 25 °C, 96.29 MHz): δ −5.37 ppm. ^{19}F NMR (CD_2Cl_2, 25 °C, 282.38 MHz): $\delta = -133.5$ (d, 12F, $J = 19.80$ Hz, o−F), −160.6 (t, 6F, $J = 19.80$ Hz, p−F), −166.0 (t, 12F, $J = 19.80$ Hz, m−F) ppm. ^{205}Tl NMR (CD_2Cl_2, 25 °C, 288.49 MHz): δ −53 ppm. Single crystals suitable for X-ray diffraction were grown as colorless blocks by recrystallization from a Et_2O/light petroleum mixture stored at −26 °C. Structural studies performed on these crystals indicated the presence of four molecules of diethyl ether coordinated to the thallium atom (compound **2b**).

Synthesis of $[Tl(OEt_2)_2][H_2N\{B(C_6F_5)_3\}_2]{\cdot}CH_2Cl_2$ (2c). Compound **1** (3.00 g, 2.5 mmol) was reacted overnight with TlOEt (0.65 g, 2.6 mmol) in dichloromethane to give a colorless solution. After workup with light petroleum in a way identical to that of **2a**, a fine white powder was isolated. Characterization by NMR spectroscopy and microanalysis of this solid, isolated in a yield of 2.73 g (74%), confirmed it to be $[Tl(OEt_2)_2][H_2N\{B(C_6F_5)_3\}_2]{\cdot}CH_2Cl_2$. Anal. Calcd for $C_{44}H_{22}B_2F_{30}NO_2Tl{\cdot}CH_2Cl_2$ (%): C, 36.58; H, 1.64; N, 0.95. Found: C, 36.24; H, 1.39; N, 0.96. ^1H NMR (CD_2Cl_2, 25 °C, 300.13 MHz): δ 5.70 (br s, 2H, NH_2), 3.64 (q, 8H, $J = 7.00$ Hz, CH_2−O), 1.29 (t, 12H, $J = 7.00$ Hz, CH_3) ppm. $^{13}C\{^1H\}$ NMR (CD_2Cl_2, 25 °C, 75.47 MHz): δ 149.8, 146.6, 141.1, 138.6, 137.8, 135.1 (all Ar−C_6F_5), 66.4 (CH_2−O), 15.5 (CH_3) ppm. ^{11}B NMR (CD_2Cl_2, 25 °C, 96.29 MHz): δ −5.33 ppm. ^{19}F NMR (CD_2Cl_2, 25 °C, 282.38 MHz): $\delta = -133.4$ (d, 12F, $J = 19.80$ Hz, o−F), −160.5 (t, 6F, $J = 19.80$ Hz, p−F), −166.1 (t, 12F, $J = 19.80$ Hz, m−F) ppm.

Preparation of $[Tl_4(\mu^3\text{-}OH)_2][H_2N\{B(C_6F_5)_3\}_2]_2{\cdot}4CH_2Cl_2$ (3). Recrystallization of **2c** from a concentrated dichloromethane solution over a perid of 2 weeks at −26 °C produced good-quality crystals of the hydrolysis product $[Tl_4(\mu^3\text{-}OH)_2][H_2N\{B(C_6F_5)_3\}_2]_2{\cdot}4CH_2Cl_2$ (**3**) as colorless blocks in low yield. These were collected and identified by X-ray diffraction. The very low solubility of **3** in chlorinated solvents precluded characterization by NMR methods. IR data for **4** (Nujol, cm^{-1}): 3610 (w), 3565 (w), 3384 (m), 3345 (m), 1647 (s), 1599 (w), 1562 (m), 1520 (s), 1458 (s), 1309 (s), 1086 (s), 1031 (w), 977 (s), 894 (m), 803 (m), 780 (m), 765 (m), 715 (m), 693 (m), 576 (w), 515 (m), 448 (s) cm^{-1}.

Synthesis of $[Tl(toluene)_n][H_2N\{B(C_6F_5)_3\}_2]$ (4a, $n = 2$; 4b, $n = 3$). Compound **2a** (2.11 g, 1.4 mmol) was dissolved in hot toluene (75 mL) upon vigorous stirring at 75 ± 2 °C, and dry argon was bubbled through the solution at this temperature for 2.5 h. A pale oily material slowly formed upon cooling to room temperature. The supernatant was removed by syringe, and the oil was repeatedly washed with light petroleum (6 × 80 mL) to afford a fine white solid which was dried in vacuo to constant weight (yield 1.30 g, 65%). Full NMR characterization and elemental analyses were performed at this stage, and all were consistent with the formulation $[Tl(toluene)_2][H_2N\{B(C_6F_5)_3\}_2]$ (**4a**). Anal. Calcd for $C_{50}H_{18}B_2F_{30}NO_2Tl$ (%): C, 42.04; H, 1.27; N, 0.98.

(47) Tjaden, E. B.; Swenson, D. C.; Jordan, R. F.; Petersen, J. L. *Organometallics* **1995**, *14*, 371−386.

Found: C, 41.60; H, 1.22; N, 0.95. ^{1}H NMR (CD_2Cl_2, 25 °C, 300.13 MHz): δ 7.38 (m, 10H, Ar−*H*), 5.70 (br s, 2H, N*H*$_2$), 2.42 (s, 6H, C*H*$_3$) ppm. ^{13}C{^{1}H} NMR (CD_2Cl_2, 25 °C, 75.47 MHz): δ 149.8, 146.6, 141.1 (all Ar−C_6F_5), 140.7 (*i*−*C*), 138.6, 137.8, 135.6 (all Ar−C_6F_5), 130.7 (*o*−*C*), 129.9 (*m*−*C*), 126.8 (*p*−*C*), 21.5 (*C*H$_3$) ppm. ^{11}B NMR (CD_2Cl_2, 25 °C, 96.29 MHz): δ −5.34 ppm. ^{19}F NMR (CD_2Cl_2, 25 °C, 282.38 MHz): δ = −133.3 (d, 12F, J = 19.80 Hz, *o*−F), −160.5 (t, 6F, J = 19.80 Hz, *p*−F), −165.6 (t, 12F, J = 19.80 Hz, *m*−F) ppm. ^{205}Tl NMR (CD_2Cl_2, 25 °C, 288.49 MHz): δ −425 ppm. Recrystallization from a toluene solution stored at −26 °C afforded colorless blocks. X-ray diffraction analysis identified these crystals as [Tl(toluene)$_3$][H_2N{$B(C_6F_5)_3$}$_2$] (**4b**).

Synthesis of [Tl(C_6Me_6)$_2$][H_2N{$B(C_6F_5)_3$}$_2$]·*x*CH_2Cl_2 (5a, *x* = 1.5; 5b, *x* = 2.5). Compound **2a** (7.82 g, 5.3 mmol) and hexamethylbenzene (5.54 g, 34.1 mmol) were dissolved in toluene (250 mL) at 75 ± 2 °C. The temperature was kept constant and dry argon was bubbled for 4 h through the reaction mixture which gradually turned very cloudy. A gray solid precipitated as the solution was allowed to cool down slowly to room temperature. These gray impurities (presumably Tl metal) were removed by filtration through Celite. The resulting colorless solution was taken to dryness to yield an off-white sticky solid which was then repeatedly washed with petroleum ether until a white powder was obtained. Extraction with dichloromethane (100 mL) followed by removal of the volatiles under vacuum yielded compound **5a** as a fine white powder, yield 5.60 g (62%). Anal. Calcd for $C_{60}H_{38}B_2F_{30}NTl$·1.5CH_2Cl_2 (%): C, 43.55; H, 2.44; N, 0.83. Found: C, 43.79; H, 2.40; N, 0.83. ^{1}H NMR (CD_2Cl_2, 25 °C, 300.13 MHz): δ 5.70 (br s, 2H, N*H*$_2$), 2.31 (s, 36H, C*H*$_3$) ppm. ^{13}C{^{1}H} NMR (CD_2Cl_2, 25 °C, 75.47 MHz): δ 149.6, 146.6, 141.2, 138.6, 137.9, 135.6 (all Ar−C_6F_5), 134.9 (C_6Me_6), 17.1 (*C*H$_3$). ^{11}B NMR (CD_2Cl_2, 25 °C, 96.29 MHz): δ −5.40. ^{19}F NMR (CD_2Cl_2, 25 °C, 282.38 MHz): δ −133.4 (d, 12F, J = 19.80 Hz, *o*−F), −160.6 (t, 6F, J = 19.80 Hz, *p*−F), −166.1 (t, 12F, J = 19.80 Hz, *m*−F) ppm. ^{205}Tl NMR (CD_2Cl_2, 25 °C, 288.49 MHz): δ −563. Colorless crystals of **5b** were obtained by recrystallization from a concentrated dichloromethane solution kept at −26 °C.

Synthesis of [Tl_2($FeCp_2$)$_3$][H_2N{$B(C_6F_5)_3$}$_2$]$_2$·5CH_2Cl_2 (6). An initially colorless solution of **4a** (0.31 g, 0.2 mmol) in dichloromethane (20 mL) instantly turned orange upon rapid addition of ferrocene (0.04 g, 0.2 mmol), and the color persisted after stirring at room temperature for 24 h. A pale orange solid was precipitated by the addition of light petroleum (60 mL). It was isolated by filtration, washed with light petroleum (3 × 70 mL), and dried under vacuum to constant weight: yield 0.20 g (86% based on Fe). Crystals suitable for X-ray diffraction were obtained as light-orange plates by overnight recrystallization from a concentrated dichloromethane solution stored at −28 °C. Anal. Calcd for $C_{102}H_{34}B_4F_{60}Fe_3N_2Tl_2$·5$CH_2Cl_2$ (%): C, 37.02; H, 1.28; N, 0.81. Found: C, 37.34; H, 1.02; N, 0.97. ^{1}H NMR ($CDCl_3$, 25 °C, 300.13 MHz): δ 5.70 (br s, 4H, N*H*$_2$), 5.35 (s, 10H, CH_2Cl_2), 4.61 (s, 30H, C_5H_5) ppm. ^{13}C{^{1}H} NMR ($CDCl_3$, 25 °C, 75.47 MHz): δ 150.0, 146.8, 140.2, 138.3, 137.0, 135.0 (all Ar−C_6F_5), 71.0 (C_5H_5), 53.8 (*C*H$_2$Cl$_2$). ^{11}B NMR ($CDCl_3$, 25 °C, 96.29 MHz): δ −3.30. ^{19}F NMR ($CDCl_3$, 25 °C, 282.38 MHz): δ = −131.4 (d, 24F, J = 19.80 Hz, *o*−F), −158.5 (t, 12F, J = 19.80 Hz, *p*−F), −164.1 (t, 24F, J = 19.80 Hz, *m*−F).

Synthesis of [Tl(dme)(Et_2O)][H_2N{$B(C_6F_5)_3$}$_2$] (8). Compound **2a** (1.00 g, 0.7 mmol) was suspended in a solution of freshly distilled dimethoxyethane (0.87 g, 9.6 mmol) in light petroleum (50 mL). The mixture was stirred at room temperature for 1 h. The white precipitate was filtered off, washed with light petroleum (3 × 50 mL), and dried under vacuum: yield 0.95 g (96%). Anal. Calcd for $C_{44}H_{22}B_2F_{30}NO_3Tl$ (%): C, 37.52; H, 1.57; N, 0.99. Found: C, 37.44; H, 1.58; N, 1.08. ^{1}H NMR (CD_2Cl_2, 25 °C, 300.13 MHz): δ 5.76 (br s, 2H, N*H*$_2$), 3.74 (s, 4H, CH_3OCH_2), 3.57 (q, 4H, J = 7.00 Hz, CH_3CH_2O), 3.55 (s, 6H, C*H*$_3$OCH$_2$), 1.23 (t, 6H, J = 7.00 Hz, C*H*$_3$CH$_2$O). ^{13}C{^{1}H} NMR (CD_2Cl_2, 25 °C, 75.47 MHz): δ 149.8, 146.7, 141.1, 138.8, 137.8, 135.3 (all Ar−C_6F_5), 72.1 (CH_3OCH_2), 66.3 (CH_3CH_2O), 59.5 (*C*H$_3$OCH$_2$), 15.4 (*C*H$_3$CH$_2$O). ^{11}B NMR (CD_2Cl_2, 25 °C, 96.29 MHz): δ −3.38. ^{19}F NMR (CD_2Cl_2, 25 °C, 282.38 MHz): δ = −131.4 (d, 12F, J = 19.80 Hz, *o*−F), −158.8 (t, 6F, J = 19.80 Hz, *p*−F), −164.1 (t, 12F, J = 19.80 Hz, *m*−F).

Synthesis of [Tl(dme)][H_2N{$B(C_6F_5)_3$}$_2$] (9). A procedure rigorously identical to that described above for **8** was followed to react **4a** (1.14 g, 0.8 mmol) with dimethoxyethane (0.87 g, 9.6 mmol) in light petroleum (50 mL) and yielded 1.01 g of **9** as a fine white powder (95%). Anal. Calcd for $C_{40}H_{12}B_2F_{30}NO_2Tl$ (%): C, 36.00; H, 0.91; N, 1.05. Found: C, 36.26; H, 1.56; N, 1.04. ^{1}H NMR (CD_2Cl_2, 25 °C, 300.13 MHz): δ 5.76 (br s, 2H, N*H*$_2$), 3.65 (s, 4H, CH_3OCH_2), 3.46 (s, 6H, C*H*$_3$OCH$_2$). ^{13}C{^{1}H} NMR (CD_2Cl_2, 25 °C, 75.47 MHz): δ 149.6, 146.3, 141.1, 138.6, 137.9, 135.3 (all Ar−C_6F_5), 71.6 (CH_3OCH_2), 58.7 (*C*H$_3$OCH$_2$). ^{11}B NMR (CD_2Cl_2, 25 °C, 96.29 MHz): δ −3.40. ^{19}F NMR (CD_2Cl_2, 25 °C, 282.38 MHz): δ = −131.5 (d, 12F, J = 19.80 Hz, *o*−F), −158.8 (t, 6F, J = 19.80 Hz, *p*−F), −164.2 (t, 12F, J = 19.80 Hz, *m*−F).

Synthesis of [Tl(diglyme)$_2$][H_2N{$B(C_6F_5)_3$}$_2$] (10). Freshly distilled diglyme (0.94 g, 7.0 mmol) was added to a colorless solution of **8** (1.40 g, 1.0 mmol) in dichloromethane (30 mL). The resulting solution was stirred overnight at room temperature and was then taken to dryness to yield a sticky oil. A white powder was obtained in a yield of 1.36 g (90%) upon washing with light petroleum (5 × 25 mL) and drying in vacuo. Anal. Calcd for $C_{48}H_{30}B_2F_{30}NO_6Tl$ (%): C, 38.11; H, 2.00; N, 0.93. Found: C, 37.99; H, 2.00; N, 0.91. ^{1}H NMR (CD_2Cl_2, 25 °C, 300.13 MHz): δ 5.76 (br s, 2H, N*H*$_2$), 3.63 (m, 16H, OC*H*$_2$), 3.42 (s, 12H, C*H*$_3$O). ^{13}C{^{1}H} NMR (CD_2Cl_2, 25 °C, 75.47 MHz): δ 149.2, 146.0, 141.0, 138.0, 137.2, 134.8 (all Ar−C_6F_5), 70.8 (O*C*H$_2$), 69.6 (O*C*H$_2$), 58.0 (*C*H$_3$O). ^{11}B NMR (CD_2Cl_2, 25 °C, 96.29 MHz): δ −3.32. ^{19}F NMR (CD_2Cl_2, 25 °C, 282.38 MHz): δ = −131.5 (d, 12F, J = 19.80 Hz, *o*−F), −158.8 (t, 6F, J = 19.80 Hz, *p*−F), −164.2 (t, 12F, J = 19.80 Hz, *m*−F).

Synthesis of [Tl(18-crown-6)$_n$][H_2N{$B(C_6F_5)_3$}$_2$]·*x*CH_2Cl_2 (11a, *n* = 2, *x* = 0; 11b, *n* = 1, *x* = 2; 11c, *n* = 1, *x* = 0). A solution of 18-crown-6 (0.50 g, 1.9 mmol) in dichloromethane (6.0 mL) was slowly added to a solution of **8** (0.82 g, 0.6 mmol) in dichloromethane (25 mL). The solution was taken to dryness after 12 h to yield a white oily material which was washed repeatedly with light petroleum (3 × 30 mL). The resulting fine white powder was dried under vacuum, and NMR and elemental analyses were consistent with the formulation [Tl(18-crown-6)$_2$][H_2N{$B(C_6F_5)_3$}$_2$] (**11a**) (yield 0.88 g, 83%). Anal. Calcd for $C_{60}H_{50}B_2F_{30}NO_{12}Tl$ (%): C, 40.65; H, 2.84; N, 0.79. Found: C, 41.38; H, 3.03; N, 0.74. ^{1}H NMR (CD_2Cl_2, 25 °C, 300.13 MHz): δ 5.76 (br s, 2H, N*H*$_2$), 3.64 (s, 48H, OC*H*$_2$). ^{13}C{^{1}H} NMR (CD_2Cl_2, 25 °C, 75.47 MHz): δ 149.8, 146.7, 141.1, 138.7, 137.8, 135.4 (all Ar−C_6F_5), 70.5 (O*C*H$_2$). ^{11}B NMR (CD_2Cl_2, 25 °C, 96.29 MHz): δ −3.30. ^{19}F NMR (CD_2Cl_2, 25 °C, 282.38 MHz): δ = −131.5 (d, 12F, J = 19.80 Hz, *o*−F), −158.8 (t, 6F, J = 19.80 Hz, *p*−F), −164.0 (t, 12F, J = 19.80 Hz, *m*−F).

Colorless blocks of [Tl(18-crown-6)][H_2N{$B(C_6F_5)_3$}$_2$]·2CH_2Cl_2 (**11b**) suitable for X-ray crystallographic studies were obtained by recrystallization from a dichloromethane/light petroleum mixture stored at −28 °C. Drying this compound under a dynamic vacuum (<0.01 mmHg) for several hours yielded [Tl(18-crown-6)][H_2N{$B(C_6F_5)_3$}$_2$] (**11c**), the composition of which was confirmed by elemental analysis and NMR spectroscopy. Anal. Calcd for $C_{48}H_{26}B_2F_{30}NO_6Tl$ (%): C, 38.21; H, 1.74; N, 0.93. Found: C, 38.29; H, 1.84; N, 0.85. ^{1}H NMR (CD_2Cl_2, 25 °C, 300.13 MHz): δ 5.74 (br s, 2H, N*H*$_2$), 3.66 (s, 48H, OC*H*$_2$). ^{13}C{^{1}H} NMR (CD_2Cl_2, 25 °C, 75.47 MHz): δ 149.7, 146.7, 141.3, 138.7, 137.9, 135.2 (all Ar−C_6F_5), 70.2 (O*C*H$_2$). ^{11}B NMR (CD_2Cl_2, 25 °C, 96.29 MHz): δ −3.30. ^{19}F NMR (CD_2Cl_2, 25 °C, 282.38 MHz): δ = −131.3 (d, 12F, J = 19.80 Hz, *o*−F), −158.8 (t, 6F, J = 19.80 Hz, *p*−F), −164.1 (t, 12F, J = 19.80 Hz, *m*−F).

Synthesis of [Tl(Bn_2O)$_{1.5}$][H_2N{$B(C_6F_5)_3$}$_2$] (12). Dibenzyl ether (1.04 g, 5.3 mmol) was added to a solution of **4a** (0.77 g, 0.5 mmol) in dichloromethane. The resulting colorless solution was stirred overnight at room temperature. The volatiles were then pumped off to

give an off-white oil. This material was purified by dissolving it in dichloromethane and reprecipitation with light petroleum. After three reprecipitations, a white oily material was obtained which on drying under vacuum afforded a fine white solid, yield of 0.6 g (78%). Anal. Calcd for $C_{57}H_{23}B_2F_{30}NO_{1.5}Tl$ (%): C, 44.41; H, 1.50; N, 0.91. Found: C, 44.72; H, 1.60; N, 0.86. ^{1}H NMR (CD_2Cl_2, 25 °C, 300.13 MHz): δ 7.50−7.41 (m, 15 H, Ar−*H*), 5.76 (br s, 2H, NH_2), 4.75 (s, 6H, CH_2). ^{13}C{^{1}H} NMR (CD_2Cl_2, 25 °C, 75.47 MHz): δ 149.8, 146.7, 141.1, 138.6, 137.8, 135.6 (all Ar−C_6F_5), 137.7, 130.1, 129.8, 129.4 (all Ar−C_6H_5), 73.9 (*C*H_2). ^{11}B NMR (CD_2Cl_2, 25 °C, 96.29 MHz): δ −3.38. ^{19}F NMR (CD_2Cl_2, 25 °C, 282.38 MHz): δ = −131.4 (d, 12F, J = 19.80 Hz, *o*−F), −158.6 (t, 6F, J = 19.80 Hz, *p*−F), −163.8 (t, 12F, J = 19.80 Hz, *m*−F). ^{205}Tl NMR (CD_2Cl_2, 25 °C, 288.49 MHz): δ −99.

Synthesis of [Tl(Ph$_2$MeN)][B(C$_6$F$_5$)$_4$] (13). A pale green solution was obtained upon the rapid addition of TlOEt (0.85 g, 3.4 mmol) to a solution of [Ph_2MeNH][B(C_6F_5)$_4$] (2.93 g, 3.4 mmol) in dichloromethane (25 mL). After 3 h, the volatiles were pumped off under vacuum, yielding a pale-green oil which was washed with light petroleum (5 × 30 mL). The resulting colorless solid was dried in vacuo to constant weight: yield 2.90 g (80%). Anal. Calcd for $C_{37}H_{13}BF_{20}NTl$ (%): C, 41.66; H, 1.23; N, 1.31. Found: C, 40.91; H, 1.25; N, 1.20. ^{1}H NMR (CD_2Cl_2, 25 °C, 300.13 MHz): δ 7.43−7.38 (m, 4H, Ar−*H*), 7.14−7.07 (m, 6H, Ar−*H*), 3.36 (s, 3H, CH_3). ^{13}C{^{1}H} NMR (CD_2Cl_2, 25 °C, 75.47 MHz): δ 150.0, 146.9, 140.5, 138.2, 137.0, 135.0 (all Ar−C_6F_5), 149.5, 131.2, 122.2, 120.8 (all Ar−C_6H_5), 40.5 (*C*H_3). ^{11}B NMR (CD_2Cl_2, 25 °C, 96.29 MHz): δ −11.70. ^{19}F NMR (CD_2Cl_2, 25 °C, 282.38 MHz): δ −131.4 (d, 8F, J = 19.80 Hz, *o*−F), −161.2 (t, 4F, J = 19.80 Hz, *p*−F), −165.5 (t, 8F, J = 19.80 Hz, *m*−F). ^{205}Tl NMR (CD_2Cl_2, 25 °C, 288.49 MHz): δ −435.

Computational Details: All calculations were performed with the Amsterdam density dunctional (ADF) program suite, version 2004.01.[41−45] Scalar relativistic corrections[48] were included via the ZORA to the Dirac equation.[49,50] The Tl valence basis set was taken from the ADF ZORA/TZP directory and employs uncontracted, Slater-type functions, of primarily triple-ζ quality, to represent the 4f, 5s, 5p, 5d, 6s, and 6p orbitals. For C and H a ZORA/DZP (double-ζ plus polarization) basis was used. The frozen core approximation was used, Tl (4d) and C (1s). The local density parametrization of Vosko, Wilk, and Nusair[51] was employed in conjunction with the PBE[52] gradient corrections. The ADF numerical integration parameter was set to 4.0 in all geometry optimizations, and the energy gradient convergence criterion was set to 1×10^{-3} au/Å. For the generation of potential energy surfaces using the "linear transit" facility, the integration parameter was set to 7.0. Mulliken population analyses were performed.[53]

X-ray Crystallography. Crystals of compounds **5b**, **6**, and **11b** were mounted on glass fibers and fixed in the cold nitrogen stream on an Oxford diffraction Xcalibur 3 CCD diffractometer equipped with Mo Kα radiation and graphite monochromator. Intensity data were measured by thin-slice ω- and φ-scans. Data were processed using the CrysAlis-CCD and -RED[54] programs. Data for compounds **2b**, **3**, and **4b** were collected similarly on a Nonius KappaCCD diffractometer and processed with the COLLECT and DENZO/SCALEPACK software.[55] For all samples, absorption corrections were applied from multiple scans of equivalent reflections.[56] The structures were determined by the direct methods routines in either the SHELXS program[57] or SIR92[58] and refined by full-matrix least-squares methods, on F^2s, in SHELXL. The non-hydrogen atoms were refined with anisotropic thermal parameters. Hydrogen atoms were included in idealized positions and their U_{iso} values were set to ride on the U_{eq} values of the parent carbon atoms. Scattering factors for neutral atoms were taken from ref 59. Crystal and refinement data are collected in Tables 2 and 3.

Acknowledgment. We gratefully acknowledge support from the Engineering and Physical Sciences Research Council. We thank Dr. Alexander Traut and Professor Josef Hahn (University of Cologne, Germany) for recording the ^{205}Tl NMR data and Dr Simon J. Coles (University of Southampton, U.K.) for assistance with the crystallographic studies of compounds **2b**, **3**, and **4b**.

Supporting Information Available: Details on the synthesis and crystal structure of [(C_5Me_5)Sn][H_2N{B(C_6F_5)$_3$}$_2$]·1.5CH_2Cl_2 and crystal and refinement data for compounds **2b**, **3**, **4b**, **5b**, **6**, **7**, and **11b**; crystal data in CIF files. This material is available free of charge via the Internet at http://pubs.acs.org.

JA0657105

(48) Kaltsoyannis, N. *J. Chem. Soc., Dalton Trans.* **1997**, 1−11.
(49) van Lenthe, E.; van Leeuwen, R.; Baerends, E. J.; Snijders, J. G. *Int. J. Quantum Chem.* **1996**, *57*, 281−293.
(50) van Lenthe, E.; Snijders, J. G.; Baerends, E. J. *J. Chem. Phys.* **1996**, *105*, 6505−6516.
(51) Vosko, S. H.; Wilk, L.; Nusair, M. *Can. J. Phys.* **1980**, *58*, 1200−1211.
(52) Perdew, J. P.; Burke, K.; Ernzerhof, M. *Phys. Rev. Lett.* **1996**, *77*, 3865−3868.
(53) Mulliken, R. S. *J. Chem. Phys.* **1955**, *23*, 1833−1841; 2338; 2343.
(54) (a) *CrysAlis-CCD;* (b) *CrysAlis-RED;* Oxford Diffraction Ltd.: Abingdon, U.K., 2005.
(55) (a) Hooft, R.; Nonius, B.V. *COLLECT*; 1998. (b) Otwinowski, Z.; Minor, W. *DENZO/SCALEPACK*; *Methods Enzymol.* **1997**, *276*; *Macromolecular Crystallography*; Carter, C. W., Jr., Sweet, R. M., Eds.; Academic Press: New York, 1997; Part A, pp 307−326.
(56) Blessing, R. H. *SORTAV*; *J. Appl. Cryst.* **1997**, *30*, 421−426.
(57) Sheldrick, G. M. *SHELX-97 - Programs for crystal structure determination (SHELXS) and refinement (SHELXL)*; University of Göttingen: Göttingen, Germany, 1997.
(58) Altomare, A.; Cascarano, G. L.; Giacovazzo, C.; Guagliardi, A. *J. Appl. Crystallogr.* **1993**, *26*, 343−350.
(59) *International Tables for X-ray Crystallography*; Kluwer Academic Publishers: Dordrecht, The Netherlands, 1992; Vol. C, pp 500; 219; 193.